

## **INFORMATION TO USERS**

**This manuscript has been reproduced from the microfilm master. UMI films the text directly from the original or copy submitted. Thus, some thesis and dissertation copies are in typewriter face, while others may be from any type of computer printer.**

**The quality of this reproduction is dependent upon the quality of the copy submitted. Broken or indistinct print, colored or poor quality illustrations and photographs, print bleedthrough, substandard margins, and improper alignment can adversely affect reproduction.**

**In the unlikely event that the author did not send UMI a complete manuscript and there are missing pages, these will be noted. Also, if unauthorized copyright material had to be removed, a note will indicate the deletion.**

**Oversize materials (e.g., maps, drawings, charts) are reproduced by sectioning the original, beginning at the upper left-hand corner and continuing from left to right in equal sections with small overlaps.**

**Photographs included in the original manuscript have been reproduced xerographically in this copy. Higher quality 6" x 9" black and white photographic prints are available for any photographs or illustrations appearing in this copy for an additional charge. Contact UMI directly to order.**

**ProQuest Information and Learning  
300 North Zeeb Road, Ann Arbor, MI 48106-1346 USA  
800-521-0600**

**UMI<sup>®</sup>**



**University of Alberta**

**A POSTURE MONITORING SYSTEM USING ACCELEROMETERS**

by

**Ralph Jay Nevins**



A thesis submitted to the Faculty of Graduate Studies and Research in partial fulfillment of the requirements for the degree of **Master of Science**.

Department of Electrical Engineering and Computer Engineering

Edmonton, Alberta  
Spring 2002



**National Library  
of Canada**

**Acquisitions and  
Bibliographic Services**

**395 Wellington Street  
Ottawa ON K1A 0N4  
Canada**

**Bibliothèque nationale  
du Canada**

**Acquisitions et  
services bibliographiques**

**395, rue Wellington  
Ottawa ON K1A 0N4  
Canada**

*Your file Votre référence*

*Our file Notre référence*

**The author has granted a non-exclusive licence allowing the National Library of Canada to reproduce, loan, distribute or sell copies of this thesis in microform, paper or electronic formats.**

**The author retains ownership of the copyright in this thesis. Neither the thesis nor substantial extracts from it may be printed or otherwise reproduced without the author's permission.**

**L'auteur a accordé une licence non exclusive permettant à la Bibliothèque nationale du Canada de reproduire, prêter, distribuer ou vendre des copies de cette thèse sous la forme de microfiche/film, de reproduction sur papier ou sur format électronique.**

**L'auteur conserve la propriété du droit d'auteur qui protège cette thèse. Ni la thèse ni des extraits substantiels de celle-ci ne doivent être imprimés ou autrement reproduits sans son autorisation.**

0-612-69743-6

**Canada**

**University of Alberta**

**Library Release Form**

**Name of Author:** Ralph Jay Nevins

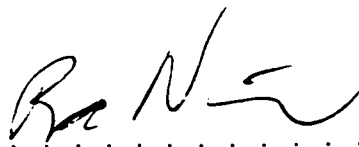
**Title of Thesis:** A Posture Monitoring System Using Accelerometers

**Degree:** Master of Science

**Year this Degree Granted:** 2002

Permission is hereby granted to the University of Alberta Library to reproduce single copies of this thesis and to lend or sell such copies for private, scholarly or scientific research purposes only.

The author reserves all other publication and other rights in association with the copyright in the thesis, and except as hereinbefore provided, neither the thesis nor any substantial portion thereof may be printed or otherwise reproduced in any material form whatever without the author's prior written permission.



.....  
Ralph Jay Nevins  
12 Donnington Pl.  
Ottawa, Ontario  
Canada, K2H 7H8


**Date:** JAU 14 2002

Let me tell you the secret that has lead me to my goal.  
My strength lies soley in my tenacity  
*Louis Pasteur*

University of Alberta

Faculty of Graduate Studies and Research


The undersigned certify that they have read, and recommend to the Faculty of Graduate Studies and Research for acceptance, a thesis entitled **A Posture Monitoring System Using Accelerometers** submitted by Ralph Jay Nevins in partial fulfillment of the requirements for the degree of **Master of Science**.

 .....

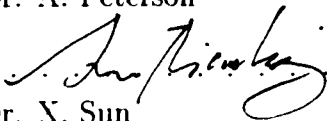
Dr. N. Durdle

 .....

Mr. J. Raso

 .....

Prof. Dr. A. Peterson

 .....

Dr. X. Sun

Date: Jan. 21/02 . . .

**To Monica, Pascale and the yet unnamed**



# Abstract

A new method of monitoring spinal posture in the sagittal plane is presented. Utilizing over sampled, low frequency filtered, accelerometer inclinations of up to six points along a subject's spine, posture is measured during activities of daily living. Data can be monitored and collected over extended periods (up to four weeks) utilizing the inexpensive, low-power, and portable data logger developed in the course of this research.

# Acknowledgements

In order of first appearance in supporting me in this endeavor or affecting my path to get where I am today:

**My mother Joan Nevins**, Prof. R.T. Pivik, Prof. Schirmer, **My wife Monica Nevins**, Prof. Vogan, The MIT Math department, Prof. Sodini, Prof. Troxel, Microsystems Technology Laboratories at MIT, Prof. Boning, The Math Department of the University of Alberta, The Department of Electrical Engineering at the University of Alberta, **My supervisor Prof. Nelson Durdle**, Prof. Duncan Elliott, My brother Lloyd Nevins, Lumic Electronics and a cast of thousands.

Many thanks to you all.

Financial and moral support of this work by Ralph Nevins & family is gratefully acknowledged.

# Contents

<b>1</b>	<b>Introduction</b>	<b>1</b>
<b>2</b>	<b>An Overview of the Spine, and Measurement Methods</b>	<b>4</b>
2.1	Scoliosis and the Spine . . . . .	4
2.2	Measurement of the Scoliosis Deformity . . . . .	8
2.3	Portable System Specification . . . . .	11
<b>3</b>	<b>Literature Review of Modern Posture Measurement and Technology</b>	<b>12</b>
3.1	Accelerometers . . . . .	13
3.2	Magnetic Sensors . . . . .	19
3.3	Mechanical Sensors . . . . .	20
3.4	Electromagnetic Sensors . . . . .	21
3.5	Summary . . . . .	22
<b>4</b>	<b>System and Software Design</b>	<b>24</b>
4.1	Accelerometers . . . . .	24
4.2	Sensors . . . . .	28
4.3	Satellite Processors . . . . .	30
4.3.1	Interrupts . . . . .	30
4.3.2	Operational modes . . . . .	31
4.3.3	Additional Features . . . . .	33
4.3.4	Theory vs Practice . . . . .	34
4.4	Master Processor . . . . .	34
4.4.1	Software – Hardware Interface . . . . .	36
4.4.2	File System . . . . .	37
4.4.3	Clocks . . . . .	38
4.4.4	Serial I/O . . . . .	39
4.4.5	Core Scheduler . . . . .	39
4.5	System . . . . .	42
4.5.1	EEPROM and Menu . . . . .	44
4.5.2	Power Consumption . . . . .	45
4.6	Data Format . . . . .	46

<b>5 Calibration and Results</b>	<b>49</b>
5.1 Calibration . . . . .	49
5.1.1 Error Correction . . . . .	54
5.2 Analysis . . . . .	57
5.2.1 Regimented Posture Data . . . . .	59
5.2.2 Unregimented data . . . . .	67
<b>6 Conclusions and Suggestions for Future Work</b>	<b>72</b>
6.1 Conclusion . . . . .	72
<b>7 Afterword (or if I had to do this again...)</b>	<b>74</b>
<b>Bibliography</b>	<b>76</b>
<b>A Master Schematic</b>	<b>80</b>
<b>B Satellite Schematic</b>	<b>82</b>
<b>C PCB Layout</b>	<b>84</b>

# List of Figures

1.1	Posture measurement system. The circle is a quarter for scale. . . . .	2
2.1	Anatomical planes . . . . .	5
2.2	Posterior and lateral views of the spine . . . . .	7
2.3	Example of Cobb angle . . . . .	9
4.1	Driven three plate capacitor into a selective demodulator. . . . .	25
4.2	Duty cycle modulated (DCM) single output of an accelerometer . . . . .	27
4.3	Sensor Schematic . . . . .	29
4.4	Duty Cycle Modulated Dual outputs of the accelerometer . . . . .	31
4.5	Simplified master processor flowchart. . . . .	40
4.6	A simplified schematic view of the posture measurement system . . . . .	44
4.7	A single sensor's data, showing the break-up of data in the hex digits . . . . .	48
5.1	Plotted ratio centers . . . . .	50
5.2	Theta and rho . . . . .	51
5.3	Polar histogram over 4 positions for the six sensors . . . . .	53
5.4	Error with projected error . . . . .	55
5.5	Sensor locations . . . . .	58
5.6	Standing with Back Against Wall . . . . .	61
5.7	Sitting in a Chair . . . . .	61
5.8	Sitting Slouched Forward . . . . .	61
5.9	Prostrate on Table . . . . .	62
5.10	Touching Toes . . . . .	62
5.11	Recline Head On Pillow . . . . .	62
5.12	Recline Face Down . . . . .	63
5.13	Rocking Chair1 . . . . .	63
5.14	Rocking Chair2 . . . . .	63
5.15	Sitting with Back Against the Wall . . . . .	64
5.16	Slouch Head Back . . . . .	64
5.17	Walking Up Down Stairs . . . . .	64
5.18	Twelve posture positions over a one hour period of regimented postures . . . . .	66
5.19	Standard deviation over a one hour period of regimented postures . . . . .	67
5.20	Spine angles over a five hour period . . . . .	69
5.21	Histograms of the corrected sensor angle over a five hour period . . . . .	70

5.22	Raw count standard deviations of X and Y sensors over a five hour period . . . . .	71
A.1	Schematic of the Master processor and CF connector . . . . .	81
B.1	Schematic of the satellite processors . . . . .	83
C.1	PCB Layout of Satellite & Master Boards . . . . .	85

# List of Tables

4.1	Specifications of the ADXL202E [1]	25
4.2	Measured $T^2$	27
4.3	Specifications of the AT90s2313 [2]	30
4.4	Specifications of the ATmega103L [2]	35
5.1	Sensor centers	51
5.2	Sensor rotation calibration	52
5.3	Sensor Positioning Error	56
5.4	Twelve regimented postures	60

# Chapter 1

## Introduction

This thesis investigates a novel method of measuring posture over extended periods. This posture measurement will occur as the subject continues their regular daily activities, and have possible applications toward monitoring idiopathic scoliosis. This measurement is accomplished by positioning accelerometers along the vertical axis of the spine in the mid sagittal plane and collecting data indicating the angles of spinal movement. The newly designed logger for this data is inexpensive, low-power, and portable (pocket-sized). Therefore the objectives are:

*Objective #1* To develop/create a facilitator for a long term study of posture, which may also be used to examine aspects of idiopathic scoliosis. This includes creating a multiuse, low power, low cost and easy to use data logger.

*Objective #2* To examine low frequency use of accelerometers to monitor spinal inclinations in the sagittal plane.

Measuring a patient's posture is an important tool in diagnosing several medical problems, such as back pain and certain spinal deformities. However, in a clinical setting or test, patients' postures may improve with their awareness of their posture, and thus give a misleading picture of the role posture plays in causing their symptoms. Hence it is important to observe their posture, and stresses and movements of the spine, during day-to-day normal activities.

One particular spinal condition under consideration is the deformity associated



with scoliosis, an abnormal lateral curvature of the spine. To date, few non invasive devices are available to measure this condition, and most are non-portable. The main motivation of this thesis was to evaluate a specific portable two-dimensional posture measurement system which could be used to monitor this condition.

Motion-position sensors have several aspects which make them ideal for monitoring the posture of patients. One of these properties is that they consume little power, which allows them to be portable and thus used with less intervention, for longer studies. Another is that they require little or no calibration, making them easy to use and extremely adaptable. They require few (or no) wires, simplifying the process of mounting the device onto the subject. An ideal sensor would have the ability to both measure angles as well as inter-sensor absolute distance; however, it is difficult to achieve both these aspects in a small, low-power device. A good design should allow the patient to correctly attach the device at home (with the help of a spouse or parent, for example) and use it as prescribed by the physician or researcher.

The posture measurement system which was created for this study is pictured in Figure 1.1. It is  $69mm \times 115mm \times 38mm$  and weighs  $250g$  including batteries. The

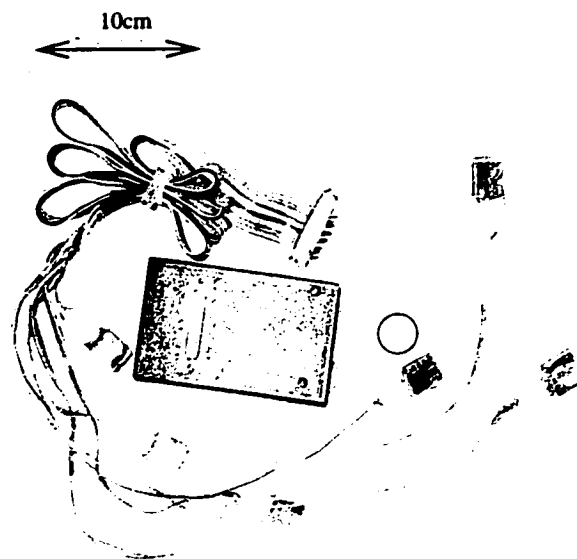


Figure 1.1: Posture measurement system. The circle is a quarter for scale.

sensors and harness wiring weigh 125g. The data logger is capable of collecting up to 32Mbytes of data which translates up to 810 hours of data (see Section 4.6). The 6 sensors are equally distributed from 100 to 152mm from the data logger. Typically, parameters for data collection are set ahead of time, and stored in the data logger until used. These parameters include the number of sensors, the amount of time between data collection, the length of the trial and others. Once the data logger is turned on (via switch 1 on the front panel) the initial parameters are read in from storage and data collection commences. If pauses or gaps are necessary in the collection, a subject may pause the collection by moving switch 3 to the “on” position on the front panel. Collection is resumed once switch 3 is placed in the “off” position.

This thesis is organized as follows.

Chapter 2 gives an overview of spinal anatomy, and defines in particular the idiopathic scoliosis spinal deformity. It then outlines the current clinical measurement techniques for idiopathic scoliosis. It discusses several potential portable measurement sensors and systems, and prefaces what led to the decision to create the current accelerometer-sensor system.

In Chapter 3, a review of relevant literature pertaining both to measurement of posture, and position measurement in general, is discussed. This review includes published reports of use of accelerometers in posture and motion studies, along with data-logging advancements.

The components and design of the final system are described in Chapter 4. In particular, the sensors, the micro-controllers, and both the hardware and software that comprise the data logger are described in detail.

The calibration of the device, and the analysis of data collected, is covered in Chapter 5. Chapter 6 concludes, with a summary of the capabilities and possible uses of the posture measurement system. It also describes, various simple extensions and or modifications that could be made to utilize the posture measurement system for other research.

## Chapter 2

# An Overview of the Spine, and Measurement Methods

This chapter provides the background and motivation for the development of a posture measurement system. The chapter begins in Section 2.1 with a clinical description of the scoliosis deformity of the spine. Measures, such as the *Cobb angle*, which are commonly used to evaluate and diagnose scoliosis, are described. Section 2.2 describes the most common methods used today for the measurement of the scoliosis deformity in a clinical setting. An outline for the specifications for a portable scoliosis-monitoring device is given in Section 2.3, as well as a brief description of a number of potential designs.

The main forms of measurement devices are those which take acoustical, optical, magnetic, inertial, or mechanical measurements. The purpose of the thesis will be to qualitatively compare these approaches and synthesize a functional unit.

### 2.1 Scoliosis and the Spine

The anatomic planes are used as a reference when speaking of the human anatomy. Figure 2.1 (Adapted from [13]) describes the division of the body into these octants.

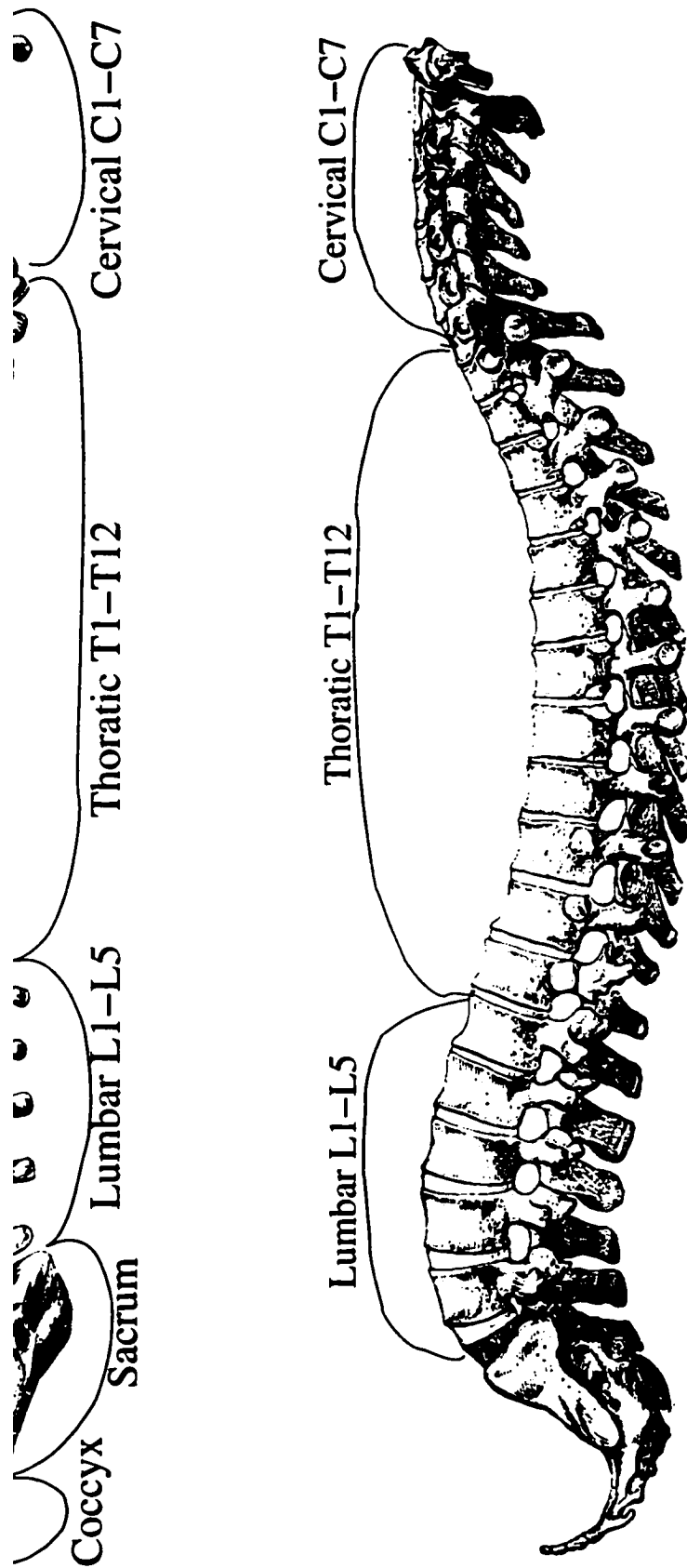
The human spine is made up of 24 vertebrae. Each vertebra is composed of the *vertebral body* in the front, the *facet joints* in the back, and the *pedicles*, which connect the vertebral body to the facet joints. The human spine is divided into three sections:

- the *cervical spine*, or neck, which is made up of 7 vertebrae (labeled C1–C7),
- the *thoracic spine*, made up of 12 vertebrae (labeled T1–T12), and
- the *lumbar spine*, or low back, which consists of 5 vertebrae (labeled L1–L5).

After the last lumbar vertebra is a mass of five smaller bones which are naturally fused together, forming a triangle. This bone mass is called the *sacrum*. Below the sacrum is the *coccyx*, or tailbone, made up of four small bones fused together. (See Figure 2.2 Adapted from [13]) While the bones and vertebrae are similar throughout the spine, each spinal section has unique attributes.

The cervical spine is comprised of the top seven vertebrae. The cervical vertebrae are the smallest of the vertebrae, and their bone tissue is denser than those in any other region of the vertebral column. The cervical spine is arranged into a sagittal curve with anterior concavity. The thoracic spine consists of twelve vertebrae, which are aligned with the curvature in the sagittal plane with posterior concavity. The thoracic vertebrae are larger than those in the cervical region and are mainly responsible for the lateral bending of the spine. The lumbar vertebrae are concave on the lateral surfaces and anterior surfaces. The lumbar vertebrae vary in size, growing larger as one descends toward the sacrum. The lumbar spine assists in carrying the weight above and provides some inherent stability to the human trunk. The lumbar spine is mainly responsible for anterior and posterior bending.

Strands of tissue called ligaments provide more coherent structure to the spine. The *anterior longitudinal ligament* extends from the occipital bone (lowest part of the skull) to the sacrum. It supports the vertebral column and unites the vertebral bodies anteriorly. The *posterior longitudinal ligament* runs on the posterior surfaces of the vertebral bodies. These ligaments extend down through the entire length of the vertebral column, and fan out at the vertebral margins to reinforce the fluid-filled intervertebral discs which separate each pair of vertebrae. *Intertransverse ligaments* connect adjacent vertebra. The articulated nature of the ligaments in conjunction



2.2: Posterior and lateral views of the spine

with the vertebrae is what gives the spine its flexibility.

Posture is studied in various ways. There are force plates, gyroscopes, goniometers, weighted potentiometers' and accelerometry covering various aspects of stance and motion. Current trend of research is to look at the spine as a single entity with one, and sometimes two sensors to monitor position. This study will be looking at spinal angles in the sagittal plane.

*Scoliosis* (after the Greek word for "bent") is a deformity of the spine which occurs to some extent in up to 10% of the adolescent population. The Scoliosis Research Society defines scoliosis as a "lateral deviation of the normal vertical line of the spine which, when measured by X-ray, is greater than ten degrees. Scoliosis consists of a lateral curvature of the spine with rotation of the vertebrae within the curve" [34]. Scoliosis is called *idiopathic* in those cases where there is no known cause; this is the most common form of scoliosis. Idiopathic scoliosis is divided into three major categories, depending on the age of onset, and varying in manifestations. The three categories are

- infantile or congenital (0–3 years),
- juvenile (3–10 years) and
- adolescent (10–17 years).

## 2.2 Measurement of the Scoliosis Deformity

The scoliosis deformity and its effects may be present in all sections of the spine, but it most commonly occurs in the thoracic spine. The most widely used measurement of scoliosis deformities is the *Cobb angle*, first described in 1948 [8]. It is used to separate scoliosis deformities into two groups: structural and functional. A *structural curve* refers to a segment of the spine with a lateral curvature that lacks flexibility. A *functional curve* refers to a curve that has no structural component and corrects or over-corrects on recumbent side-bending roentgenograms.

To determine the Cobb angle, one must specify the upper and lower limits of the curve which have the maximum tilt toward concavity. If lines are drawn parallel to the upper end plate of the upper body and parallel to the lower end plate of the lower body (see Figure 2.3 adapted from [13]), the Cobb angle is defined as the acute angle between the lines.

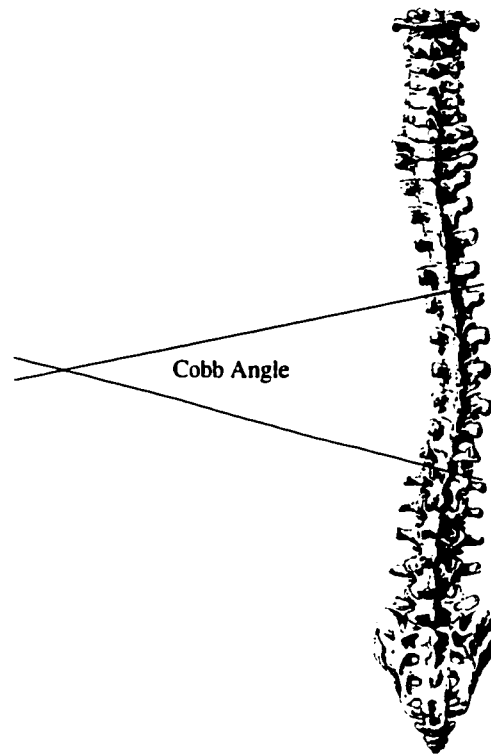


Figure 2.3: Example of Cobb angle

The severity of scoliosis is split into three general categories based on the Cobb angle, the spinal maturity of the patient and the physical age of the patient. When the Cobb angle is less than  $10^\circ$ , the scoliosis is considered mild, and in most cases the deformity is within the bounds of normal spinal curvature. In these cases therapeutic intervention is not necessarily considered. When the Cobb angle is between  $25^\circ$  and  $40^\circ$ , the scoliosis is considered moderate and therapeutic intervention in the form of braces is generally recommended. If the Cobb angle is greater than  $50^\circ$ , the scoliosis is considered severe and surgical therapeutic intervention may be recommended [33].

Note that the measurement of the Cobb angle is generally an invasive technique, due to the use of ionizing radiation to capture the images needed to determine this angle. Moreover, it is only a one-dimensional view of the lateral deformity of the spine. It is not possible to determine rotational aspects of the vertebra with accuracy using a single plane view [36].

There are several techniques that use ionizing radiation to measure aspects of scoliosis (such as the Cobb angle) in clinical settings. These methods include CT scans, bi-plane radiographs and single-plane radiographs. Although accurate, use of these methods must be limited to restrict radiation exposure. CT scans are taken with the patient in the supine position; whereas patients may be placed in any position for radiographs. Bi-plane radiographs are realized as stereo or 90° radiography. Although single-plane radiographs give a far less complete picture, they are often used for their comparative low cost and low radiation dose.

On the other hand, techniques such as Magnetic Resonance Imaging (MRI) give as much information as a CT scan, but without the radiation risk. The prohibitive aspect of MRI is its limited availability and high cost.

Other important, non-invasive, measurement techniques are more cosmetically oriented and deal with back surface measurements. For instance, some back surface measures are optical in nature. These include moiré topography, line and point projection, and scanning. These measures involve projecting light from one location and measuring — photographically, videographically, or via variations in reflected intensity — from another location. Moiré topography is a passive method, realized as, for example, topographic photogrammetry, in which the patient is illuminated with a point source which is passed through a grating. This illumination causes a fringe pattern to be projected on the patient's back. Minor variations of movement cause dramatic changes in the fringe patterns [31]. However, studies of this nature are fraught with interpretation problems.

Line scanning methods have claimed depth resolutions of up to  $0.5mm$  [15], but



have slow sample times: to the order of  $750ms$  [41], and up to 1 second using phase-measuring profilometry [12]. These slow times cause an introduction of artifact due to physiological functions that occur on the same time scale, with the same magnitude of movement (*eg.* breathing, heart rate).

## 2.3 Portable System Specification

While highly accurate and informative, none of the techniques (invasive or not) described in the last section are portable, nor are they appropriate for continuous or repeated measurements. They are limited in use to the clinical environment, where they help to define the seriousness of the deformity.

One of the objectives of this thesis was to design a portable measuring device which could be used by physicians to monitor spinal posture. To design a useful, convenient portable posture measurement system, several items must be considered:

- the placement of the sensors to maximize information pertaining to scoliosis
- the types and quality of information to be obtained
- the speed and cost of processing the data
- the overall quantity of data (in samples/minute)
- ease of use.

These aspects of the posture measurement system are discussed in the following chapters.

## Chapter 3

# Literature Review of Modern Posture Measurement and Technology

In this chapter a review of the current literature regarding a class of inertial sensors with a view toward determining their applicability to the thesis goals; namely, to create a portable device to monitor physiological posture positions during day to day activities. A class of inertial sensors that are examined are those having both low cost and low power. Also of interest are sensors that can be used and operated by untrained personnel.

The sensor used in such a device should be low power, since the goal is to apply it to a portable long-duration investigation of posture. This necessitates low current consumption and a low-duty-cycle type of device.

The low-cost property is necessary for the adoption of such a device in mainstream practice. The cost depends not only on the cost of the one sensor, but also on the type of sensor and the type of measurement, and thus the number of sensors necessary to construct the device. Other components also drive the cost. If the cost of the device used to record the sensors' output was an order of magnitude higher than the sensors, variation in sensor cost would not impact future studies as much.

All of the sensors examined in this chapter are inertial sensors. An inertial sensor is one in which the sensor is at rest with respect to its immediate surroundings, but

free of external influence in observations. That is, it gains all information from forces that act upon the whole frame of reference uniformly rather than (for example) a near point source.

Since sensors that could operate during ambulatory activities of daily living, only inertial sensors can be considered. Inertial sensors allow the device to be either self-referenced or to use an external reference that acts upon the whole frame equally. A self-referenced system would have to depend on constant diminishing of a physical property or a mechanical connection. Examples of a diminishing physical property include an electromagnetic field or a magnetic field. An externally referenced system needs to observe a globally physical property to be able to make a position assessment. Examples of such a physical property include gravity and the Earth's magnetic field.

This chapter is divided into several sections, each corresponding to a different class of sensor. In each section, relevant articles from the literature, and the methods in light of the goal of a portable, low-cost, low-power measurement device evaluated. Section 3.5 concludes with an overall review of the state of the field as uncovered by this literature review, and summarizes some of the more promising ideas found.

### **3.1 Accelerometers**

In this section, accelerometers, which are inertial devices which function with respect to the Earth's gravitational field are considered.

Accelerometry has been used to study the kinematics of human body segments for almost fifty years. Currently, inertial devices are used in the fields of Virtual Reality, medical monitors and robotics. Accelerometry does not give absolute position or linear measure. It does provide information that can be used to understand the environment of the subject and their posture. In particular for subjects at rest, accelerometers can function as inclinometers.

A variety of accelerometer transducers including piezoelectric, force feedback and strain gauge were available for use in early studies. Each of the three have significant

problems for their application to kinematics. Older piezoelectric accelerometer transducers respond when a set point has been reached. Force feedback transducers are prohibitively expensive, and some strain gauges have elasticity deformation problems.

Morris's 1973 paper [29] describes one of the earliest uses of a semiconductor cantilever accelerometer in a human movement study. Five accelerometers were used on a platform molded to a subject's shank, that is, to the area on one leg between the ankle and the knee. The purpose of the study was proof of concept: that a cantilever accelerometer could be used in a human study. He also used a digital computer to interactively analyze the transducer data; quite remarkable for the time.

With the hopes of achieving functional neuromuscular stimulation (FNS) — restoring standing and mobility functions by stimulating muscles — thigh and shank motion analysis becomes critical. The detection of different stages of stance and leg motion is integral to the development of such a system. The studies that examine leg motion attempt to detect four distinct phases: stance, push off, swing and landing contact. Prior methods, utilizing goniometers instead of accelerometers, had been error prone.

The first of these studies was conducted by Foerster et al. [11]. Although their stated claim was to attempt detection of posture and motion by accelerometry, the actual study was smaller in scope, attempting only to classify posture into one of several categories. A main impetus for the paper was to attempt to correlate other health related functions (eg., heart rate, respiration and blood pressure) to posture position. The sensors used were a packaged product with a full-scale reading of  $2g$  that was integrated with the commercial recording device. In the study, four sensor placements were used: sternum, wrist, thigh, and lower leg. Data for calibration were collected from nine different postural activities both prior to the experimental period and afterward. During the experiment, data were collected for a 50 minute time period while the observer suggested various activities to the subject. The activities were noted and monitored for time in order to be correlated with data collected. It should be noted, however, that this was not a correct blind test, as the monitor

was potentially the same for each subject and also potentially the same person who analysed the data; there is nothing in the article to suggest otherwise. Nevertheless, the results of this paper suggest that it is possible to make classifications of postural activities utilizing accelerometers.

Another such study, conducted by Bouten [6], describes human body acceleration. Commercially available tri-axial accelerometers were used with an off-the-shelf data logger. All experimentation on the subjects was done in a “respiration chamber”, that is, a room (with all amenities) functioning as a metabolic chamber, where respiratory gas exchange could be measured exactly. Accelerometers were calibrated using a speed-controlled lathe to induce centrifugal forces on each axis. Within the confines of the experiment, subjects sat, ran and exercised within the respiration chamber. The subjects did not venture outside of the lab and only performed set duties in a very controlled environment. While the experiment seems to have been very well thought out, there was a curious lack of control subjects and the author made few objective claims. For instance: the accelerometers were only attached in one location; it was claimed that the accelerometers would not influence the subject’s activities; and no group was monitored to test with no accelerometers attached. The robustness of such a sensor data-recorder arrangement is not known.

Laden and Wu [19] developed a system utilizing a tri-axial accelerometer and LED system. They were studying thigh and shank movement in a normal walking gait. The leg data were correlated utilizing a tethered data recorder with video monitoring software and a tracking program. In later studies ([51] and [52]), Wu et al. incorporated an angular rate accelerator. The studies use a low pass filter of 100 Hz on all acceleration data. Previous studies (by different authors) had indicated that 5-7 Hz would be adequate, but Laden and Wu found that there was indeed an amount of power being released in a normal gait at 12 Hz.

A large volume of work related to accelerometry, covering a range of topics, has been published out of the University of Twente (The Netherlands). Functional neuro-

muscular stimulation (FNS) was the focus of a number of these studies by Willemsen [50], [49], Veltink [46] and Heyn [14], concentrating specifically on leg movement. These studies attempt to typify the stages of limb movement in a normal walking gait. Four accelerometers, two on each thigh and two on each shank, were used to monitor the subjects' gaits. In one such study, the authors tested accuracy by comparing against a goniometer, while in the others, a video system is used. Calibration of the accelerometers remains a problem. One study by Lotters et al. [21] from Twente attempts to define a particularly interesting procedure for use in calibration. Most studies in the literature utilize a tri-axial accelerometer in a typical right handed coordinate system. This tends to be a problem as the z axis measure holds near zero during most daily activities. The error on these measurements is thus often greater than the calculated values when determining the absolute position of the actual sensor with respect to the Earth's gravity. It is possible through error analysis to correct for this by placing the tri-axial accelerometers in a rotated coordinate system. This places the most sensitive area available in the most active area of measurement for the three transducers. This interesting calibration technique may be applicable to other types of sensors.

Another use of accelerometry data is in standing stability tests. One set of experiments, by Mayagoitia et al. [26], placed both a force plate and an accelerometer at the height of center of mass (COM) to monitor a subject's movement during predetermined activities. The study determined that the accelerometer was able to distinguish between different test conditions with the same accuracy as the force plate. The results of another study (Waarsing et al. [47]) suggest that a performance parameter which can be calculated from the data gleaned from the accelerometer can order different gait patterns according to stability. Another study in the same vein, conducted by Mayagoitia et al. [25], utilized a true portable system in which the data were saved to a palm top computer. More study was indicated. The authors hope that such data can be used to monitor the progress of a therapeutic intervention of a progressive

disease.

In the area of rehabilitation, objective analysis of static and dynamic daily activities may improve treatment. To that end, a study by Veltink et al. [44] utilized a small set of uniaxial accelerometers to attempt to distinguish several activities. These activities included sitting, lying, walking, ascending stairs, descending stairs and cycling. The study was conducted in a controlled environment. The three accelerometers used were placed tangentially on the thigh, radially on the sternum and tangentially on the sternum. The experimenters found that they were indeed able to distinguish between dynamic activities based upon mean signal and signal morphology. Baten et al. [5] used a single accelerometer as well as a gyroscope to estimate back load in ambulatory subjects. The data collected was validated against a 3D video-based motion analysis system. The inertial system estimated the absolute back inclination angle with an error of  $\pm 10\%$ . As is often the case when using micromachined accelerometers, temperature stability could have increased the overall accuracy.

Another Twente study, conducted by Luinge et al. [23], used a miniature gyroscope in conjunction with three uniaxial accelerometers to obtain a relative estimate of human orientation. The study showed that utilizing both types sensors for orientation gave considerable improvement over the use of accelerometers alone, although considerable drift still persisted.

Two other interesting applications of accelerometers coming out of the Veltink laboratory in Twente were reported as a hand held dynamometer to be used for kinematic sensing [43] and a method of kinematic quantification of Parkinson's bradykinesia.

The dynamometer utilized both a gyroscope and a single accelerometer in two methods of testing. For the first method — after a static period in which the the accelerometers provide an estimate of shank angle — the joint angle is estimated by integrating the gyroscope signal after an offset correction. The second method assumes that the knee joint is not linearly accelerating during the rotation of the

shank. This view pretends the shank is a pendulum and that the tangential and radial components of the actual acceleration at a position upon the shank can be estimated by placing a gyroscope at the same position. Results for the first method show that there was too much drift after a period of 10 seconds. However, the second method does imply that the knee joint does not rotate (i.e. make side movements) and that the thigh remains virtually stable.

The bradykinesia (defined as slow execution of movement) study[45] utilized tri-axial accelerometers mounted on Parkinson's afflicted patients. The objective of these measured movements was to evaluate a drug treatment of the afflicted group. Power analysis could possibly have been used to make a more quantifiable estimate if this sensor was truly feasible. As it was, the authors concluded that indeed the tri-axial accelerometer system was a useful measure in the analysis of bradykinesia for near-static circumstances.

A few years prior to the bradykinesia study, Van Someren [42] wrote about actigraphic monitoring of movement and rest activity rhythms of aging sufferers of either Alzheimer's or Parkinson's disease. Actigraphy is the long term assessment of wrist movements. The study covered two main areas. First was an objective filtering scheme to assess movement-induced accelerations. Secondly, was an alternative method to assess both the duration and intensity of movements. The author determined that a bandpass of 0.25 to 11 Hz strongly reduced gravitational artifacts and was appropriately sensitive to the age decrease in activity. Other than the filtering comments, the paper had few conclusions and was almost completely self referenced, a summary paper of previous work.

One aspect of using accelerometers is the quantification of the accelerometer-human interface. In most studies, the accelerometer and platform containing whatever wiring and interface circuitry is held onto the human body by means of Velcro straps, or cinch belts or glue type interfaces. These fastening devices dampened the response of the sensors, and introduced a systematic error into the data. Since the



transducer measures the acceleration of itself the skin-transducer interface has some elasticity. In a study at the University of Guelph conducted by Lafortune [24], a tri-axial accelerometer was mounted on the external end of a traction pin implanted in a subject's tibia. Measures of 2.7 – 3.7g during walking and 10.6g during running were observed. Data were obtained from a single subject walking and running on a treadmill. A comparison with a skin-mounted sensor demonstrates the dampening and the phase shift of such a mounting. The invasive technique used here seemed extreme, but it did provide insight into and comparison with the skin-mounted sensors.

A study done at Ritsumeikan University by Kurata et al. [18] monitored joint motion of the elbow. Tri-axial accelerometers were set on the forearm and upper arm near the elbow joint. The actual study used a mechanical model (with only one axis of rotation) to model the elbow. In fact, only a single subject was used to validate the experiment. Accelerometer noise dominated the results at small angles. There is no mention of temperature related drift hampering this study as has been the case in so many others.

An interesting device was noted by Nakahara et al. [30]: a portable accelerometer system. The accelerometers were mounted on either side of subjects' eyeglass frames to measure head acceleration. To measure trunk acceleration, the accelerometers were mounted on the left and right of a waist belt. The novel aspect of the paper is the programmable logic array (PLA) which held the timers for the accelerometers which have an acceleration pulse width modulation (PWM) output and the microprocessor interface to a PCMCIA bus, which allowed the storage of a large amount of data.

## **3.2 Magnetic Sensors**

Magnetic sensors can be used as position, distance and angular data collectors. Usually in close proximity to the source of the magnetic field, Hall sensors need high field strengths to operate. Over the past 20 years, a new type of magnetic sensor has been developed utilizing the planar Hall effect. Other types of magnetic sensors are

included in this survey, as well, offering different possibilities and points to ponder.

In a study conducted by Baltag et al. [4], an interesting tilt sensor was developed using a magnetic fluid (ferrofluid). The fluid is captive in a partially filled 12cm long tube with  $153\text{mm}^2$  cross sectional area. A primary coil covers the entire length of the tube. A center-tapped secondary coil is constructed over the primary, such that half of the secondary coil is placed at either end of the device. The induced voltage on the secondary is proportional to the tilt on the longitudinal axis. The phase of the induced voltage changes when the longitudinal axis passes 0 and  $180^\circ$ .  $0.01\text{mm}/\text{m}$  accuracy was obtained — though not in the presence of a great deal of vibration.

A simple direction sensor based on a Hall sensor was written up by Bramanti and Tozzi in [7]. They describe a method of detecting and monitoring the ambulation of a patient along a specified pathway. The study measured deviations as low as  $1^\circ - 2^\circ$ . This was only defined to function on a specified pathway parallel to the magnetic field of the Earth.

The third magnetic system that is discussed, was developed by Kadushkin et al [17], involves a giant magnetoresistive (GMR) type of sensor that has a distance measure of up to  $\pm 25\text{cm}$ . This magnetodiode was found to have linear regions of sensitivity and a lot of temperature independence. The Russian paper was written in 1987, yet there does not appear to be any follow-up of this promising measurement device.

### 3.3 Mechanical Sensors

In the scope of this review, mechanical sensors were initially left off the list of inertial sensors. However, an intriguing (and possibly applicable) device of this kind was uncovered in the literature.

Roduit et al [32] constructed a novel mechanical device to measure angles using a pair of cables. The cables were anchored at one end. The angular change could be calculated by measuring the distance between the two free ends when the cables

are bent along different paths. This cable system is particularly interesting due to its temperature stability, low power and low calibration requirements. The measured accuracy of the system was  $\pm 2^\circ$  on a stroke of  $100^\circ$  and a resolution of less than  $0.1^\circ$ . A temperature dependence of less than  $0.2^\circ$  per  $^\circ C$ . The device is compared successfully against a goniometer and other measurements “found in the literature” (none are cited).

Another aspect touched upon briefly in this paper is the possibility of a three-dimensional sensor based upon three cables, although no study or construction was done.

### 3.4 Electromagnetic Sensors

In this section, a review of the use of tri-axial electromagnetic sensors in the PhD thesis of Edmond Lou[22]. The tri-axial coil method is fundamentally easy yet numerically difficult. It is a proven technique and clinical studies are in progress.

Edmond Lou produced an interesting measurement system that utilized two sets of three tri-axial coils to transmit and receive a pulsed signal. The strength of the signal could then be measured and from that measurement, the distance between the transmitter and receiver could be calculated. The system as described was accurate to  $1.1^\circ - 4^\circ$  from  $0^\circ - 90^\circ$ . It also compared favorably to a commercial system. The data analysis, however, is computationally intensive and must be done off line.

The coils were wrapped in three axes on a cube, made of ferrite for a higher gain. The receiver coils were tethered to the processing unit by the power and buffered signal return cable. Overall power consumption was  $550mW$  per day at an initial sample rate of 15 minutes between samples. This device was verified against a camera-based measurement system.

It does appear that some signal conditioning might have been saved by having the transmitter coils remote rather than the receiver coils. A self contained transmitter needing only an enable signal — three distinct enables or two encoded enables —

power and ground wires could have been constructed. This could have reduced the necessary signal noise and buffering problems associated with the distant receivers.

### **3.5 Summary**

The aforementioned studies demonstrate the successful use of accelerometers in a posture measurement system. All the studies above used sensors in motion based studies, that is, monitoring rapid joint movement during activities. The goal of this thesis is to examine data which averaged over short intervals to obtain static “snapshots” of average spinal posture. This has not been done previously.

The concept of offsetting (rotating) the accelerometers to gain accuracy can be transplanted into other systems. Also studies that use data loggers for long term storage can be considered and refined.

The literature shows that accelerometers are indeed temperature-sensitive devices[5][18]. This sensitivity would have to be overcome or circumvented if accelerometers were to be used in a long term study. The advent of micromachined capacitance-based accelerometers does reduce the drift that plagued many of the early studies that utilized piezoelectric accelerometers.

As stated previously, accelerometry does not give absolute position or linear measure. It does, however, provide other information that can be used to understand the environment of the subject and their posture, in particular the angle of incline to the vertical.

As microelectronic processes improve, the potential for a sensor fusion — multiple sensors of different types — may be the next step in human motion and position monitoring.

As previous literature shows accelerometers can be used in two ways. Either as a short term, fast movement activity, removing the Earth’s gravitational force mathematically to get actual forces exerted on joints, or as a slow inclinometer, a type of sensor that returns actual tilt of an object. It is the latter aspect of accelerometers

**that will be utilized within this study.**

# Chapter 4

## System and Software Design

In this chapter, a bottom-up approach is used to discuss the design of the system and the software. Sections 4.1 and 4.2 contain a detailed analysis of the accelerometers and the sensor assembly used. In Section 4.3, the *satellites* are described, which are the microprocessors and software that control the sensors and collect the data. Following this is Section 4.4, with the description of the *master processor*, which controls the satellites, collects the data and saves it to the storage device. The system as a whole is covered in Section 4.5, discussing all remaining aspects, and finally Section 4.6 gives a look at the format in which the data is saved.

### 4.1 Accelerometers

There are several types of accelerometers which would be appropriate for this research, including mercury, resistive, cantilever and capacitive. Each of the aforementioned sensors have the ability to measure tilt and have accurate angle sensitivity. This study used a capacitive model ADXL202E, because of its extremely small size, high accuracy, low-power, low-voltage attributes and availability. See Table 4.1 for accelerometer attributes.

These micro-machined (iMEM) accelerometers with integrated electronics are built from an etched polysilicon plate, which forms the center plate of a three-plate capacitor. The plate is suspended in such a way as to move only in the sensed di-

<b>ADXL202E</b>
2-Axis Acceleration Sensor on a Single IC Chip
5mm × 5mm × 2mm Ultrasmall Chip Scale Package
2mg Resolution at 60 Hz
Low-Power $\leq 0.6mA$
Direct Interface to Low-Cost Microcontrollers via Duty Cycle Output
Bandwidth Adjustment with a Single Capacitor
3 V to 5.25 V Single Supply Operation
1000 g Shock Survival

Table 4.1: Specifications of the ADXL202E [1]

rection (that is, in the opposite direction of the acceleration vector), toward one or the other of the two end-plates. On each side of the suspended plate are two fixed comb structures that the plate’s “fingers” fit into (see Figure 4.1). The ADXL family of accelerometers measures this motion by determining the change in the difference between the two capacitances. This change in difference is directly related to the distance moved.

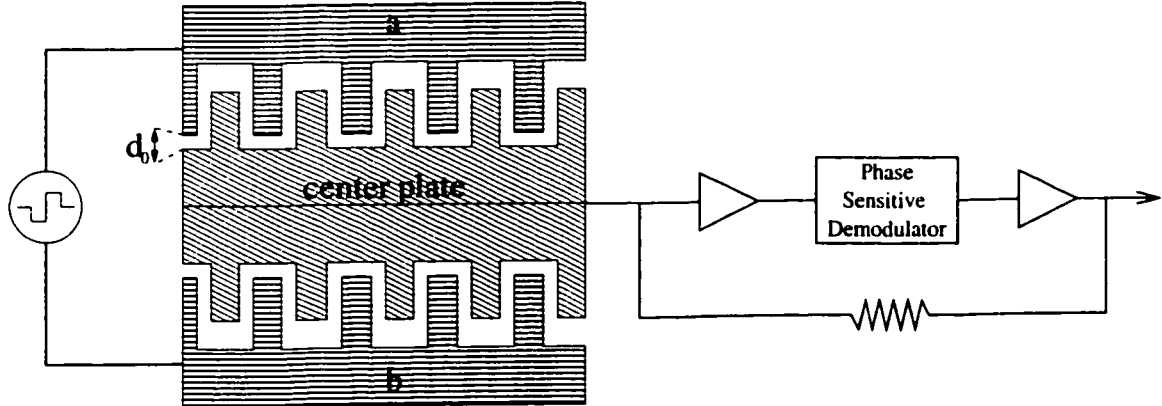


Figure 4.1: Driven three plate capacitor into a selective demodulator.

As described by Stilson [37]; when the center plate is at rest, it is (theoretically) equidistant from the two capacitors; denote the spacing between the plate and the capacitors by  $d_0$ . Thus each of the two capacitors, having the common center plate, has an capacitance of  $C = \frac{k}{d_0}$ , where  $k$  is determined by the properties of the plates (such as the active surface area and the composition of the plates). As the plate

moves a distance  $\Delta d$  towards plate  $a$  (and thus the same distance away from plate  $b$ ), the capacitance of each pair changes as

$$C_a = \frac{k}{d_0 - \Delta d} \quad \text{and} \quad C_b = \frac{k}{d_0 + \Delta d},$$

or equivalently,

$$C_a = C \frac{d_0}{d_0 - \Delta d} \quad \text{and} \quad C_b = C \frac{d_0}{d_0 + \Delta d}.$$

The resulting difference in capacitance between the two capacitors is

$$\Delta C = C_a - C_b = C d_0 \left( \frac{1}{d_0 - \Delta d} - \frac{1}{d_0 + \Delta d} \right) = \frac{2C d_0 \Delta d}{d_0^2 - (\Delta d)^2}.$$

Consequently, the differential capacitances across the capacitors' fingers are proportional to  $\Delta d$ , for small values of  $\Delta d$ .

These differential capacitances across the capacitors' fingers are detected by the signal-conditioning portion of the accelerometer. The two outer fixed combs are driven by square waves  $180^\circ$  out of phase. An acceleration will unbalance the plate capacitance by  $\Delta C$ , and the resulting square wave amplitude will be approximately proportional to the distance travelled by the suspended plate, and hence to the magnitude of the acceleration. The onboard demodulation of the rectified square wave determines the direction of the acceleration.

Thus, the output of the ADXL202E is a Duty Cycle Modulated (DCM) signal whose duty cycle (that is, ratio of pulsewidth to period) is proportional to the acceleration detected. This allows for a strictly digital design in determining acceleration. More precisely, acceleration in the axis can be deduced, by computing the ratio  $= T1/T2$ , where  $T1$  is the pulsewidth and  $T2$  is the period of the cycle (a relatively constant value). See Figure 4.2. The range of the possible values obtained is centered at  $x_0 = 0.5$  (theoretically, but not in practice; see Section 5.1). Thus, a vector representing the acceleration is obtained in the axis of acceleration by taking the difference  $x - x_0 = \bar{x}$ .



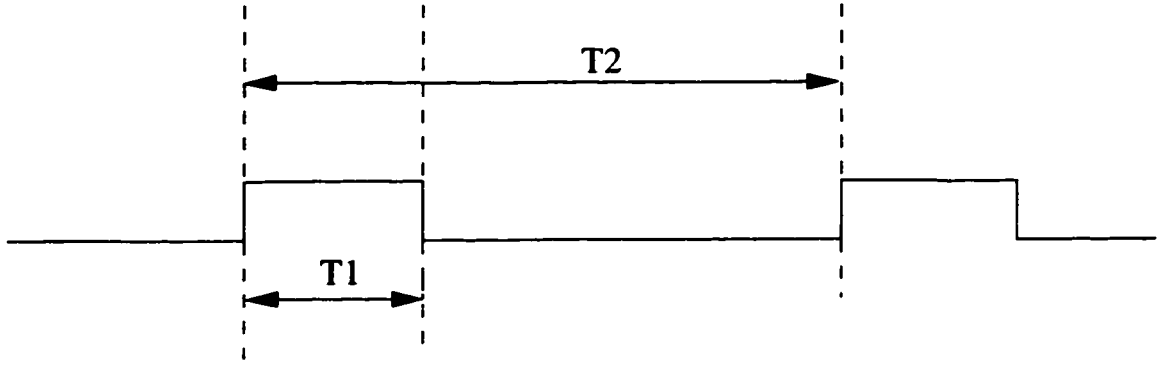


Figure 4.2: Duty cycle modulated (DCM) single output of an accelerometer

The assumption is made that accelerations on the body (other than gravity) are in general much smaller than one gravity. Hence the signal and resulting vector is only dependent on the orientation of the sensor with respect to gravity. The accelerometer then becomes an inclinometer. That is, the two sensors at a right angle on the ADXL202E can deduce its position by summing their respective vectors and subtracting the known offset due to gravity.

Operating parameters for this research targeted a resolution of tilt less than  $0.5^\circ$ . This resolution had to fit within the capabilities of a 16 bit counter, at a clock speed of 3.6864 MHz. The counter was not prescaled thus a maximum count of  $\frac{65535}{3686400} = 0.0711$  seconds can be allowed. The measured period of  $T2$  versus a sample of mean counts can be seen in Table 4.2. Column one is measured values of  $T2$  for

Sensor	$T2(ms)$	mean (count)	Calculated $T2(ms)$
1	4.57	16922.3	4.59
2	4.59	16964.8	4.60
3	4.19	15485.1	4.20
4	4.23	15859.2	4.30
5	4.60	16961.3	4.60
6	4.40	16232.2	4.40

Table 4.2: Measured  $T2$

the six sensors. Column two holds satellite measured mean of counts of  $T2$  that over done 3268 periods. The calculated  $T2 = \frac{count}{3686400} (ms)$  values (column three) are within 0.6% of measured values (column one).

A bandwidth of 50Hz,  $F_{-3db}$  or slower was targeted for the accelerometers. The sample period for  $T2$  is to be greater than twice that value, less than 10ms, to satisfy nyquist sampling limits. This still allows for a wide variation of the 16bit counter from sample to sample. Under these bandwidth conditions, a standard deviation calculation from the saved data can provide information which could be used to typify movement or qualify the data.

To determine the size  $C$  of the capacitors, one for each accelerometer in the package, necessary to achieve this bandwidth, the following formula from the ADXL202E specification sheet is applied:

$$C = \frac{1}{2\pi 32k\Omega \times F_{-3db}}.$$

A value of  $F_{-3db} = 50Hz$  yields  $C = 0.1\mu F$ .

The value of  $0.1\mu F$  was found to be convenient, it was also the same value as the decoupling capacitor  $C_{DC}$ . To calculate  $T2$  the following  $T2 = \frac{R_{set}\Omega}{125M\Omega}$  was used. A slow value of approximately 5ms was targeted to allow a maximum count from the 16bit counters. A common value of  $R_{set} = 620k\Omega$  was used to provide a  $T2 = \frac{620k\Omega}{125M\Omega} = 4.96ms$ .

Other design considerations that fell under the timing of  $T2$  was that some value  $N$  was required to fit within the memory confines of the satellite processors. This memory constraint prevented  $T2$  from growing greater than 14 bits of usable data in the limited data space of the processors. If  $T2$  had grown or if there was more accuracy desired, i.e. 15 or 16 bits, the amount of buffered data of the satellite processors would have had to be reduced.

## 4.2 Sensors

The six sensors used were Analog Devices model ADXL202E. Each sensor comprises of two accelerometers in perpendicular axes (denoted  $X$  and  $Y$ ). The sensors are surface mountable, and the active  $X$  and  $Y$  axes of the chip are parallel to the

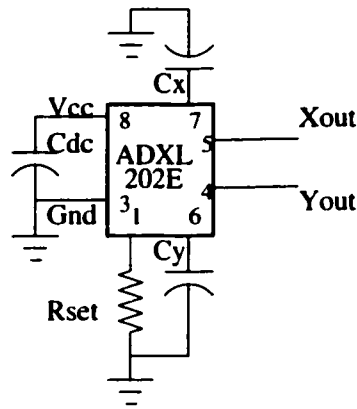


Figure 4.3: Sensor Schematic

standard mounting plane.

The components of a sensor are shown in Figure 4.3.

For the current study, alternate mounting procedures had to be considered since the plane of interest was perpendicular to the standard mounting plane. Thus, the devices were mounted in a trench  $1\text{mm}$  wide drilled on a piece of  $0.1''$  gridded phenolic board. These boards measured  $15\text{mm} \times 15\text{mm}$ , and held the other passive components necessary for operation. Five of the six sensors were mounted at an angle so that the most accurate portion of the sensors' range would be attained when the subject was upright (sitting or standing). The remaining sensor was mounted with its axes in the "upright" direction, approximately  $45$  degrees from the others.

Since all analog conversion is done within the sensors themselves, only digital data is output. Decoupling capacitors were provided on each sensor assembly. All sensor assemblies were hand-wired and then encased in a plastic resin to protect them from moisture and mechanical stresses. Finally, each sensor assembly was supplied with a keyed lockable 4 pin connector to provide power, ground and return sensor X and Y DCM data to a processor.

<b>AT90s2313</b>
118 Powerful Instructions Most Single Clock Cycle Execution
32 x 8 General-purpose Working Registers
2K Bytes of In-System Programmable Flash
128 Bytes of SRAM
128 Bytes of In-System Programmable EEprom
One 8-bit Timer/Counter with Separate Prescaler
One 16-bit Timer/Counter with Separate Prescaler
On-chip Analog Comparator
Programmable Watchdog Timer with On-chip Oscillator
SPI Serial Interface for In-System Programming
Full Duplex UART
Low-power Idle and Power-down Modes
External and Internal Interrupt Sources
Fully Static Operation
Power Consumption at 4 MHz, 3V, 25C
Active: 2.8 mA
Idle Mode: 0.8 mA
Power-down Mode: $\leq 1\mu A$
15 Programmable I/O Lines
2.7 - 6.0V (AT90S2313-4) 0 - 4 MHz (AT90S2313-4)

Table 4.3: Specifications of the AT90s2313 [2]

## 4.3 Satellite Processors

Each sensor assembly is associated with a satellite processor whose function is to process and collect the output from the sensors, and then relay this data on to the master (main) processor in efficiently sized packets. For this research, an AT90s2313 model was chosen. The ATMEL AT90s2313 processors were chosen as satellite processor because of the size of the RAM, the low voltage/low current capability, 16 bit timer and the on-board UART. An additional bonus was the ease of use and simple instruction set. See Table 4.3 for the specifications of this processor.

### 4.3.1 Interrupts

The data output from the accelerometers is asynchronous in nature, so a low-latency interrupt is necessary. The AT90s2313 has two “interrupt-on-change” pins (denoted

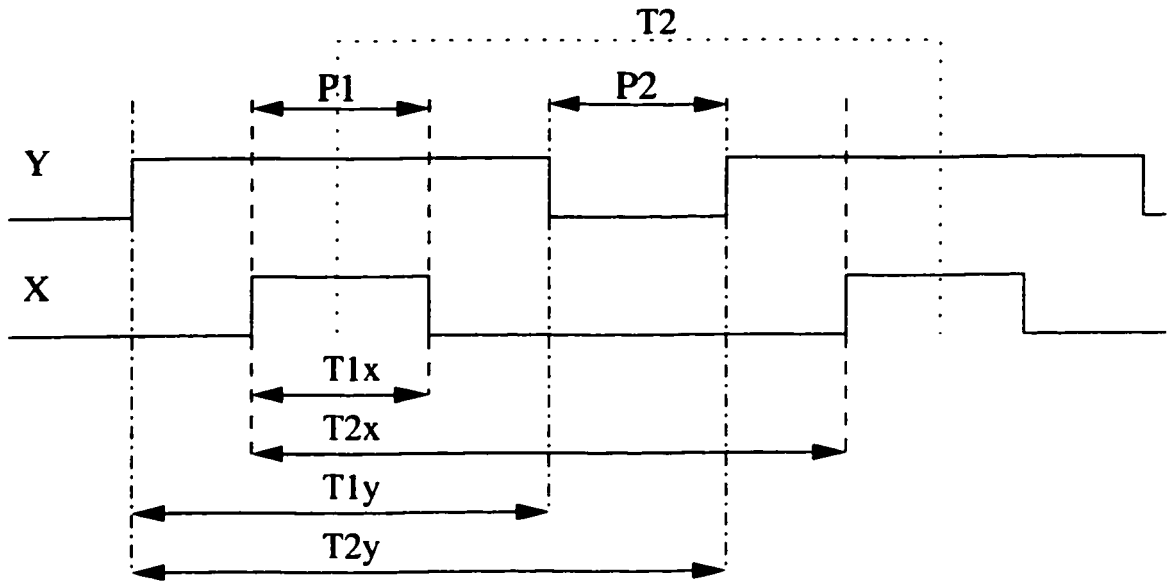


Figure 4.4: Duty Cycle Modulated Dual outputs of the accelerometer

INT0 and INT1). These allow a low-maintenance interrupt process. To decrease the latency, the number of instructions performed within each interrupt routine is kept to a minimum, and no interrupt is allowed to occur within another. Interrupts always occur in pairs, one for each of X and Y DCM. The accelerometers signals are time-locked to the centers X and Y when high and low.

The interrupt latency is 4 cycles for the initial measurement, and, in worst case, 14 cycles if the interrupt occurs within the 10 cycles during which the previous interrupt is serviced.

All timing routines are based on the 3.6864MHz clocks utilizing the 16 bit timer to measure the DCM signals.

### 4.3.2 Operational modes

All satellite processors are held in reset mode until signaled to start by the master processor. Once active, the satellite processors have three operational states: *run*, *buffer* and *transfer*. The two latter states are determined by the master processor,

which sends a signal along a serial line common to all satellite processors.

The highest priority of the satellite processor is to measure the pulse widths  $T1$  and the periods  $T2$  (the run state). Lower priority processing (which includes the buffer and transfer states) is done during the signal processing windows. These *windows* are the periods where both  $X$  and  $Y$  are high ( $P1$ ) and where both  $X$  and  $Y$  are low ( $P2$ ). See Figure 4.4. Each of these windows will last a minimum of 20% of the period of the cycle (and not more than 80%), thus allowing a predictable interval where no interrupts will occur.

### **Run State**

In the *run state*, data from the sensor were sampled and transferred to the initial operational buffers. Note that the buffering and transferring states occur only in intervals where no data is being received; thus the running state accepts *all* data from the sensors for the duration of the experiment. There are four pieces of data:  $T1x$ ,  $T2x$ ,  $T1y$  and  $T2y$ , and each is a 16 bit value. To obtain an average of each of these values over an *epoch*, the values are summed each iteration to give a cumulative total. This total is a 32 bit value. Moreover, to allow post-processing calculation of the standard deviation on this average (and thus a measure of the validity of the data), the  $T1$  values are squared (into a 32 bit value) and their sum is accumulated (as a 48 bit value). Finally, the count  $N$  of readings taken in each epoch is updated.

### **Buffer State**

In the *buffer state* (signaled from the master processor by the character "C" to all satellites), all accumulated data is converted into ASCII, and a checksum is computed. This ASCII data, together with the checksum, is then written into the transfer buffers, and the operational buffers are cleared to begin a new epoch.

## Transfer State

The *transfer state* is signaled from the master processor by a unique identifier to each satellite. The satellite processor acknowledges receipt of its identifier by sending an “@” on the serial line. It then proceeds to transmit its ASCII buffer data to the master processor, at a rate of one character per window. Data transmission requires no processor intervention (that is, no interrupts), and so the processor may go into “sleep mode” and wait for run state interrupts as this transmission continues. The data transmission of a single character is complete by the next processing window. Data is transmitted at 19200 baud to the master processor. Low voltage serial protocol was used to facilitate debugging, as the line can be tapped to monitor the transmitted data.

During this time, all non-active satellite processors hold their transmit lines in tristate mode to avoid bus contention. In other words, the port is only enabled on the satellite once it recognizes its identifier, and disabled once it has completed its transmission of buffered ASCII data along the shared serial line.

### 4.3.3 Additional Features

Failure of sensors is accommodated by timer overflow interrupts. These interrupts are used to prevent system failure even in case of sensor failure or wire breakage.

Additional instructions that can be passed to the satellite processors include *self reset*. This command places the processor into a hold state until signaled to restart by the master. This is an alternative to allowing the satellite processors to run for unchecked periods, which would cause the registers to overflow and become corrupted.

Extra output lines (PB0-7) on the satellite processors were used in a debugging capacity until the final code was programmed into the devices. These lines can be used as “point reached” indicators and monitored using an oscilloscope or logic analyzer.

All satellite processors were programmed off board and tested before being socketed. Each satellite processor has a *testing mode* that allows free running data collec-

tion (for a preset epoch). This testing mode was used to typify and test functionality of the satellite processors prior to installation.

All satellite processors were programmed in assembly language.

#### **4.3.4 Theory vs Practice**

Initial estimates based on the data sheets[1] for the accelerometers and estimated code complexity suggested that the satellite processors would spend approximately 40% of the time in active mode and 60% in sleep mode. These estimates were found to be conservative as the satellite processors have been found to spend greater than 80% of the time in sleep mode in the current implementation.

Though the application note for the sensors [48] from Analog Devices gives a complete method for obtaining data from a similar sensor and microprocessor setup, this method only provides a maximum of one sample for every two periods. This would not have been adequate for the chosen bandwidth (50Hz) of the devices, and therefore an implementation of a more direct method for obtaining data on every rise and fall of the DCMs was used.

The method in the application note also only computes  $T2$  periodically, presuming that its value will be constant. However, temperature variations do affect this value, and thus the results will be more accurate when  $T2$  is measured as frequently as  $T1$ . That is to say,  $T1$  will vary with  $T2$  as temperature changes, thus measuring both will provide better accuracy than measuring  $T1$  often and  $T2$  occasionally. This feature is what allows this device to overcome the temperature dependency problem discussed in Section 3.5.

### **4.4 Master Processor**

The master processor is a ATmega103L, manufactured by ATMEL; see Table 4.4 for its specifications. The main features of this processor which made it ideal for this research were the onboard 4K of static RAM (an unusually generous amount



for processors of this size) and the low cost of the development tools. It also has 6 byte-wide I/O ports, 5 of which were used in this study. Note that this processor is in the same family as the satellite processors.

<b>ATmega103L</b>
121 Instructions, most are Single Clock Cycle Execution
32 × 8 general-purpose Working Registers
128K Bytes of In-System Programmable Flash
4K Bytes of SRAM
4K Bytes of In-System Programmable EEprom
Two 8-bit Timer/Counters with Separate Prescalers
One 16-bit Timer/Counter with Separate Prescaler
Real-time Counter (RTC) with separate oscillator
8-channel ADC
Programmable Watchdog Timer with On-chip Oscillator
Master/Slave SPI Serial Interface
Full Duplex UART
Low-power Idle and Power-down Modes
Fully Static Operation
Power Consumption at 4 MHz, 3V, 25C
Active: 5.5 mA
Idle Mode: 1.6 mA
Power-down Mode: $\leq 1\mu A$
15 Programmable I/O Lines
2.7 - 3.6V 0 - 4 MHz

Table 4.4: Specifications of the ATmega103L [2]

The master processor is responsible for collecting, and verifying the checksum of, the sensor data from the six satellite processors, and writing this to a storage device. The storage device chosen was Compact Flash type 1, because it is small, can store 100's of megabytes of data, and is a common technology (with readers available for most Operating Systems and computers). In order to use the Compact Flash efficiently in this fashion, a DOS-compatible filesystem was created and used (see Section 4.4.2). Thus, in essence, the master processor software accomplished five basic tasks:

1. Hardware access to the Compact Flash the Software – Hardware Interface,

2. Access through common disk operating calls to the File Allocation Table (FAT) based DOS file system,
3. Real Time Clock (RTC) and time function,
4. Serial I/O communications, and
5. Core scheduler.

In the following five sections each of these are examined in detail.

#### **4.4.1 Software – Hardware Interface**

The hardware interface consists of the low-level access routines to the Compact Flash. The code for this interface was modified from an existing source [35]; this assembly code, based on 8051 processor, was for lowlevel access to Integrated Drive Electronics (IDE) drives only. The code that was used was status, error, low level sector read and write routines. All original assembly language code was converted to “C” or inline assembly language and complemented with debug statements.

Compact Flash devices have three modes of operation. In one of these modes (True IDE Mode), the Compact Flash emulates its motorized cousin, the IDE drive. Using this mode, the code base could be made very general, and thus reusable for other applications and storage devices (such as a common IDE drive). These base functions are the simplest, lowest level communication to the IDE interface. These comprise of functions such as `ide_read_byte`, `ide_write_byte`, `status` and `reset`.

The Compact Flash is attached to the processor through its unique CF connector. Signal routing to the connector from the master processor was accomplished through ports A, C and D. Although the ATmega103L has external bus interface capabilities, it is only an 8 bit bus, and would require an external bidirectional buffers/latches to use at 16 bits (the interface to the Compact Flash). Thus, in the interest of keeping the board area and parts-count down, a 16 bit interface was used, but only port

driven. The CF specification [9] and the ATA-2 specification [53] do allude to an 8 bit interface for conforming devices. In later specifications (ATA-4 [38], ATA-5 [39]) this mode is depreciated; therefore 8 bit addressing was not done. The time required to write to the Compact Flash card by the Master processor was not a pressing issue, therefore a sixteen bit polled interface was found to be a functional choice.

#### 4.4.2 File System

The file system code allows simplified `open`, `close`, `read`, `write`, `delete` and `find` functionality. This compatibility with the DOS FAT file system allows the rapid exchange of data from the Compact Flash to the experimenter's computer, and ease of subject operation. Initial investigation into simpler file-system methods were thwarted by high memory requirements, an existing code base too poorly documented to be adapted correctly and quickly, and cost.

The code for this DOS FAT file system was modified from one main source [10], which was originally designed for accessing floppy drives up to 1.44Mbytes only. To adapt the code to the current application, a number of modifications needed to be made. The first of these was the integration of the partition table information into the program (using [28],[27] as references), so that a higher capacity storage device (such as the Compact Flash) could be used. All personal computer (PC) specific code had to be modified, and all assembly language rewritten. A key aspect to this code was the small memory footprint as it requires only a single buffer.

"FAT12" is implemented in the current code. This effectively limits the size of the Compact Flash used to 32 MBytes. Additional modifications to allow "FAT16" (up to 540 MBytes) could be implemented with further investment of time and testing (see Section 7).

Finally, note that although `read` and `find` functionality is included, these routines were only used during testing. They are not directly used by the final embedded program, but are used indirectly through cluster map and allocate look-ups. The

internal functions of `read` and `find` were used heavily enough that the small footprint of the higher level subroutines were left for completeness.

### 4.4.3 Clocks

The Real Time Clock (RTC) ticks once every second, using a 32.768 KHz external crystal as its time base. The RTC is the controlling clock for all larger operations within the scheduler, such as waiting for epochs. The RTC is an interrupt-driven “volatile variable” tick which wakes the processor while it is waiting in sleep mode. The master processor should not be considered a “Real Time System” because not all interrupt latencies are known, nor do they need to be known. Exact timing is only critical near the end point of an epoch, when there is a fixed amount of time to service an interrupt, arising from the arrival of data along the serial line.

The only circumstances under which the master processor would not have a sufficient amount of time at this point is where at least two satellite processors have timed out (indicating some serious problems with the hardware). In such a case, all future data may be suspect if the epochs are not long enough to allow this delay before the next round of data is ready to be transferred. If the system does not have enough time at this point, (set by the operator prior to the data run), it could be indicative of a problem with two or more satellite processors. An indication of this would be erratic flashing of the “heartbeat” LEDs.

The other clock used is one of the other built in timers in the processor. It is set to run as an independent one-shot timer of 50ms. This period is used for various independent timing functions. One of these is a “heartbeat” LED, which is flashed on for typically 50 msec each second to indicate to the user when the device is operating and collecting data. Another use is to wait out the (minimal) lead time needed by the satellite processors to enter and complete their “buffer state”, and thus be ready to accept the command to enter their “transfer state” (see Section 4.3.2). Finally, the satellite processors need some settling time to release the serial bus (if necessary,

the last processor is not waited upon) and to acquire the serial bus when they are selected.

#### **4.4.4 Serial I/O**

Serial I/O routines were retrieved from an AVR forum Internet site [3]. These routines were modified to allow transparent character received semaphores, setting a flag so any sleep based timing routines are not interfered with. Serial routines are interrupt-driven and buffered, so the throughput of the satellite traffic can be captured effectively. These serial routines were used extensively during debugging, as they came complete with various data to ASCII translation facilities.

#### **4.4.5 Core Scheduler**

The core scheduling routine of the master processor is comprised of several nested loops. Control of the number of runs, the number of files per run and the number of epochs occur around these loops.

Initialization is done prior to entering the main outer loop. Within the initialization section, the UART, the file system, the IDE interface and the timers are set up. If the system is freshly loaded, or the system change switch is “on”, a menu system is called up to allow the user to define the basic program parameters of the run. These parameters include number of channels, number of seconds per epoch, the number of epoch per file and the number of files per run. See Section 4.5.1. These parameters are then written to the internal eeprom and thus saved even during power down; this allows the device to be set up remotely and then subsequently used without external input.

#### **Outer loops**

Each group of epochs defined by user input has an associated file. To insure that files are written consecutively and that there is coherence in the subject data, this file

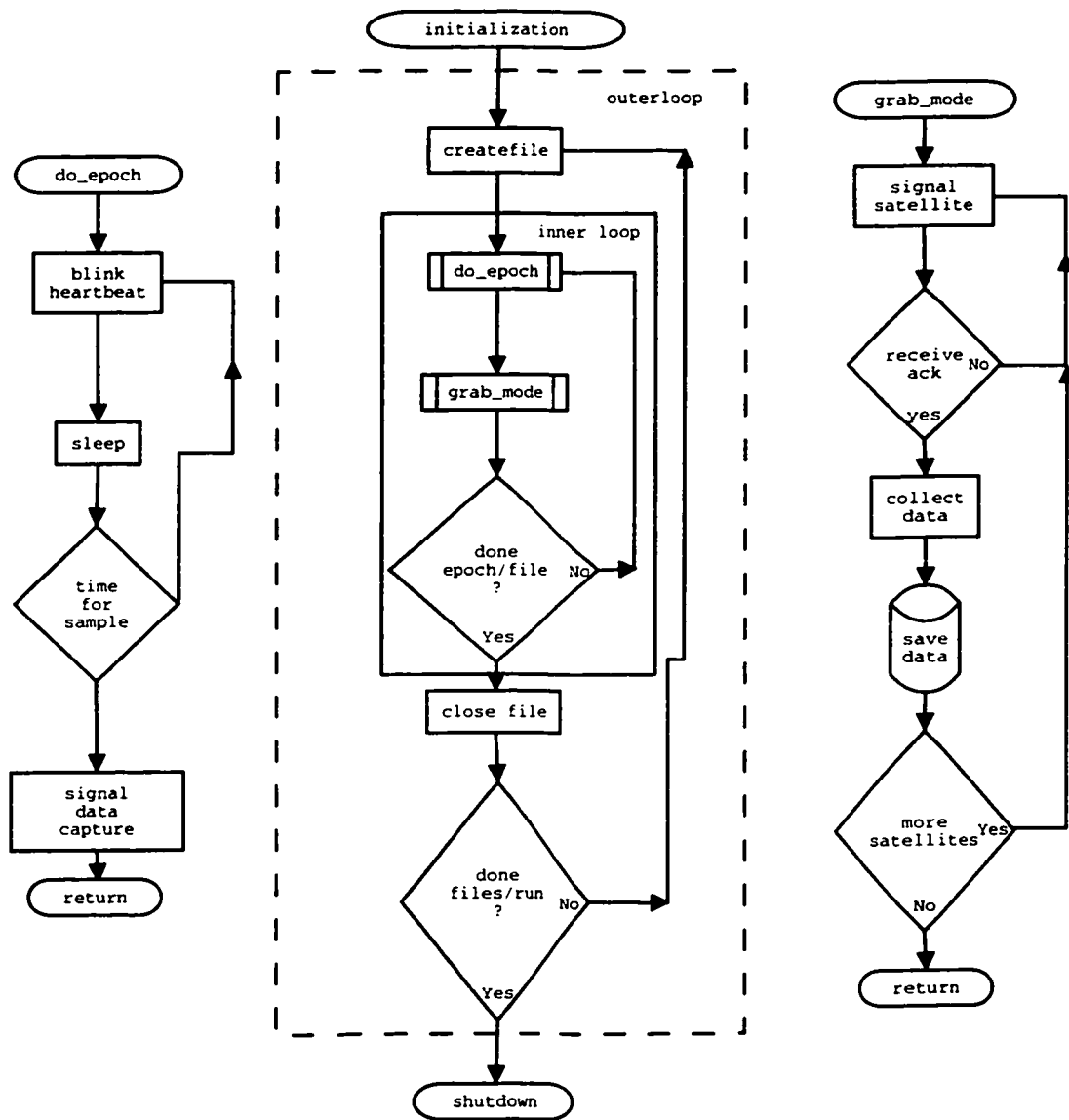


Figure 4.5: Simplified master processor flowchart.

is deleted prior to opening. Files are numbered consecutively, with a separate value used for “run”, thus there could be up to 1000 (0-999) files and 1000 (0-999) runs ; but in actuality the total number of files depends on the type of file system and the size of the Compact Flash. For example, a 4 MByte Compact Flash can hold a maximum of 120 files in the root directory on a “FAT” file system; an 8 MByte can hold approximately 250 files in the root directory. The absolute maximum number of files in the root directory is 511, which again is a “FAT” file system constraint. Note that subdirectories have no restriction on the maximum number of files though do take longer to access because it must search for available sectors the “FAT” .

In the outer loop file names are generated, files created, and after control is passed back from the inner loop, files are closed. See Figure 4.5.

### **Inner loops**

The inner loop timing is based on the number of epochs. The main function calls of the inner loop are to `do_epoch` and `grab_mode` which time and collect data.

The first of these functions, `do_epoch`, puts the master processor into sleep mode, suspending all other functions on the chip, while waiting in a tight loop for the correct number of RTC ticks (seconds) to pass. The length of this wait is called the length of the *epoch*, whose value is determined by the operator and saved to the eeprom at the beginning of the run. It is within this waiting loop that the “heartbeat” LED is flashed (see Section 4.4.3); this is done while the processor is “awake” and checking to see if the epoch is over.

Upon completion of the epoch, the satellite processors are sent the signal to enter their buffer state. Since there are no other interrupts occurring within the system, the buffering signal (a character “C” sent to all the satellites) will be sent, and will thus be acted upon within the next  $P1$  or  $P2$  time period. In the worst case, the maximum is approximately 3ms or half of  $T2$ , for the satellites to calculate periods based on the last cycle.

The call to `grab_mode` collects, checks and saves the data. The function `grab_mode` is also built out of loops which iterate over the number of channels selected to collect data from (typically all six).

In each iteration, a satellite is selected and called to send data with a unique identifier. Once the selected satellite responds, the master processor again enters a tight sleep loop as it collects the transmitted data. (As noted in Section 4.3.2, this transmission is relatively slow. One character every  $\frac{T_2}{2}$ .) The data is buffered as it arrives to allow post-collection processing. If a complete set of data is received from a satellite, its integrity is tested by means of the transmitted checksum. The data is then appended the currently open file in the Compact Flash.

A number of safety checks prevent lock-up of the system from sensor, satellite, or transmission failure. In particular, if any satellite fails to respond within three seconds, it is flagged in the file by a channel identifier (so that the operator can track which channels were not received) and the next channel is signaled. In addition, if the data stream from a given satellite fails to complete, a watchdog timer flags the channel as bad. Finally, if the checksum calculation fails to match the received value, the channel is also flagged to denote poor data.

This process is then iterated over each of the remaining channels. Once all sensors are complete, control returns to wait for the next epoch length or returns to the outer loop of the program.

## 4.5 System

The system is comprised of seven independent microprocessors on two boards. The master processor board contains the ATmega103L, the compact flash connector and user interface connectors; the other board contains the six satellite processors, where each one is dedicated to a single sensor. These two boards split the tasks of the system. The master processor board controls timing, data storage and has the I/O ports for user interface. The six processor board has sensor inputs, voltage regulation



and brown-out control. A simple schematic of the system can be seen in Figure 4.6, as shown X and Y are duty cycle modulated (DCM) sensor signals from the sensors into the satellite processors; see Appendices A and B for the detailed schematics.

Communication between the boards takes place through a stacked 10 pin connector carrying regulated power, serial I/O, and reset signals. A battery backup port is provided, allowing one to compensate for main battery failure.

Each of the seven processors is clocked through a separate 3.6468 MHz crystal. The master processor has an additional 32.768 kHz crystal to clock its Real Time Clock. The design of this double-sided board and the design of the footprints of the components (see Appendix C) was done using Protel [20]. Fine pitch surface mount components were attached using traditional soldering techniques under high magnification.

One design change, a modification of master-satellite communications, necessitated one series of rework surface wiring. An unused board-to-board pin was used for this rework.

Internal to the ATmega103L is an 8 channel analog-to-digital converter. This was not used, but was wired out/brought out to the headers on the master board to allow for future expansion of the device, or for use of the board with other kinds of sensors.

Internal flash programming of the program memory is done through the 10 pin port on the front of the assembled device. This interface port is also used to communicate to the device to program the eeprom using a standard dumb terminal and the built in menu system. This interface also provides debugging information through the receive and transmit lines of the processor. It is thus possible to monitor all communications between master and satellite processors. To do this, two separate receive lines from the device box are required, as are level converters (for example, Maxim's MAX232 or MAX2332) to translate the 0-3.3 VDC levels to standard RS232-specified voltages (minimally  $\pm 7$  VDC). The level converters could have been internally powered from the 10 pin port. External power that was used during development, and was connected

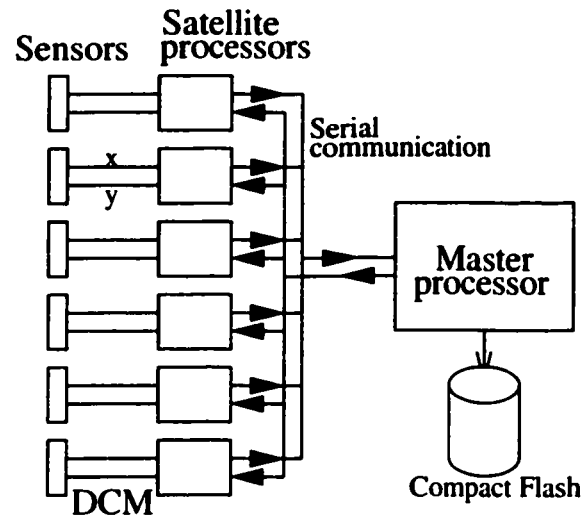


Figure 4.6: A simplified schematic view of the posture measurement system

to a bench supply when needed.

#### 4.5.1 EEprom and Menu

The menu system is active when switch 4 is in the “on” position or when the master processor has been freshly programmed. The following text box shows the setup prior to eeprom programming.

### General Guide for data collection rates

number of channels must be between 1-6  
minimum time per channel is 1 sec  
time is incremented in 1 second periods  
upper limit for an epoch is dependent on  
sampling freq.  
seconds per epoch changes the granularity of  
the data  
epoch per file may be equated to min per hour  
Ideal: 60 seconds /epoch and 60 epochs/file  
files per run may be equated to hours per day

Number of channels to be used [6]:

Number of seconds per epoch [15]:

Number of epoch per file [40]:

Number of Files per Run [60]:

Number of runs [1]:2

Your settings are :

Number of channels to be used :6

Number of seconds per epoch :15

Number of epoch per file :40

Number of Files per Run :60

Number of Runs :2

is this correct y/n [y]:y

*Channels to be used* is the number of sensors to be active. *Seconds per epoch* is the number of seconds between data collection times. The number of *epoch per file* are the number of lines which go into a file, this equal to  $(\text{number of channels}) \times (\text{seconds per epoch})$ . *Number of Files per Run* is part of the number that is assigned to the file as a file name. Likewise *Number of runs* is also part of the number that is assigned to the file as a file name.

## 4.5.2 Power Consumption

Power is supplied by four NiMh 1200mA-hr 1.2 volt cells in series. Prior research [22] [16] suggested that these would be the best possible type of battery for our purposes. These batteries are held in a 4-cell holder. The power was regulated down to the requisite 3.3 volts by an SMT linear regulator [40]. Brown out reset protection was

provided by another device which contains battery backup provisions. The battery back up was brought out to the edge of the board but was not implemented in the current version. Maximum static current was calculated (in mA) as:

$$\begin{aligned} &6 \times 1 \text{ sensors} + 6 \times 2.8 \text{ AT90S2313} + 5.5 \text{ ATmega103L} + (\text{effectively}) 0 \text{ CF} \\ &= 6 + 16.8 + 5.5 = 28.3 \text{ mA} \end{aligned}$$

During all non-active time the processors were in an idle/sleep mode which reduced the current to a theoretical  $6 \times 1 \text{ sensors} + 6 \times 0.8 \text{ AT90S2313} + 1.6 \text{ ATmega103L} = 16.3 \text{ mA}$ . Further internal service reductions (turning off unused portions of the microcontrollers) reduced running current. Actual running current was measured as an average of 15.1 mA, a power consumption of 49.8 mW. The peaks in current when writing to the Compact Flash were measured as 35 mA for a period of less than 0.5 ms; this occurred once per write cycle or, for the calibration and experimental trials, every 15 seconds. Current peaks of the “heartbeat” LED’s were so small as to be undetectable.

## 4.6 Data Format

Data are grouped into between one and six lines, depending on the number of sensors chosen for the study. For the preliminary observed subject, all six sensors were used.

Data are collected in epochs, which have a maximum duration of 4.5 minutes, due to the buffering capability of the satellite processors. Note that 240 epochs take up approximately 100K bytes of storage space. Therefore the maximum amount of amassed data that could fit in a common 4 Megabyte Compact Flash would be the equivalent of 810 hours — more than a month of continuous recording time. The minimum duration of an epoch should be four seconds plus the number of channels used; or a minimum of 5 seconds for one channel and 10 seconds for the six channel configuration. These minimal epochs allow the user to obtain a fine-grained analysis. Note that the data can easily be combined into larger epochs later, to conduct a coarser

analysis. Consideration of the size of the epoch must be weighed with prolonging battery life — the more often data is saved, the higher the current drain.

As discussed in Section 4.1, the raw data from the sensors measures, in each of two axes (X and Y) the intervals  $T1$  and  $T2$ . It is the ratio  $T1/T2$  which yields the value of the acceleration vector in a given axis. The  $T2$  periods are relatively constant, and so to obtain an estimate of the standard deviation of the data during an epoch — and thus, a measure of how variable the data was over that epoch — it suffices to compute the sum of the squares of the  $T1$  periods.

Consequently, each sensor produces one line of data per epoch. Each line of data contains both the X and Y components for that sensor for the duration of the epoch. The line is composed of 8 ASCII fields (see Figure 4.7), which are described from left to right as follows:

- (4 bytes) the count of the number of  $T1$  periods involved in the statistic
- (8 bytes) the sum of the  $T1$  periods for X
- (12 bytes) the sum of the squares of the  $T1$  periods for X
- (8 bytes) the sum of the  $T2$  periods for X
- (8 bytes) the sum of the  $T1$  periods for Y
- (12 bytes) the sum of the squares of the  $T1$  periods for Y
- (8 bytes) the sum of the  $T2$  periods for Y
- (2 bytes) the checksum value of the string.

This data are collected and written to the Compact Flash throughout the run. Once the data are moved off of the Compact Flash, post processes is done. Post processing entails splitting the data into manageable chunks for a numerical processing program (such as MATLAB) to read in comfortably. This post processing program

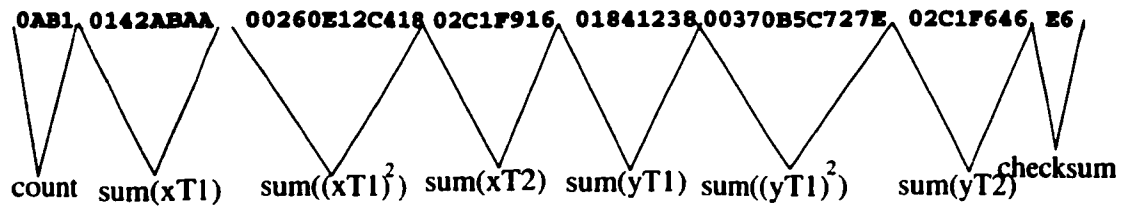


Figure 4.7: A single sensor's data, showing the break-up of data in the hex digits

was written in C. It accepts strings in the above format and produces lines composed of space-separated floating point values, as well as carrying out the initial calculations of ratio and standard deviation.

# Chapter 5

## Calibration and Results

### 5.1 Calibration

Calibration of this device was a two-step process, of which the first step was comprised of three phases. This first step was conducted immediately after construction, whereas the second step involved a test subject.

#### Step 1, Phase 1

During the first phase of the initial calibration, all of the sensors were affixed to a solid beam. The beam in turn was attached to a 100 step stepper motor about its center, with three sensors on each half of the beam. The beam could thus be rotated through an angle of  $360^\circ$  in  $3.6^\circ$  increments. Thus, the sensors were rotated counterclockwise through  $360^\circ$  in  $3.6^\circ$  steps and then “unwound”, that is, rotated clockwise through to  $0^\circ$  in  $3.6^\circ$  steps. At each step, the unit was held stable for 2 minutes. Data were collected in 15 second epochs, to ensure the collection 6 stable periods for each step. Data were collected continuously over a period of 30 hours = 1800 minutes = 7200 epochs. This allowed a net comparison of 5400 epochs — 540 at each stepped position. The program to control the stepper motor was written in C.

The resulting data were screened using the standard deviation measures of the epoch to remove the artifacts and motion corruption. This results in a measure of

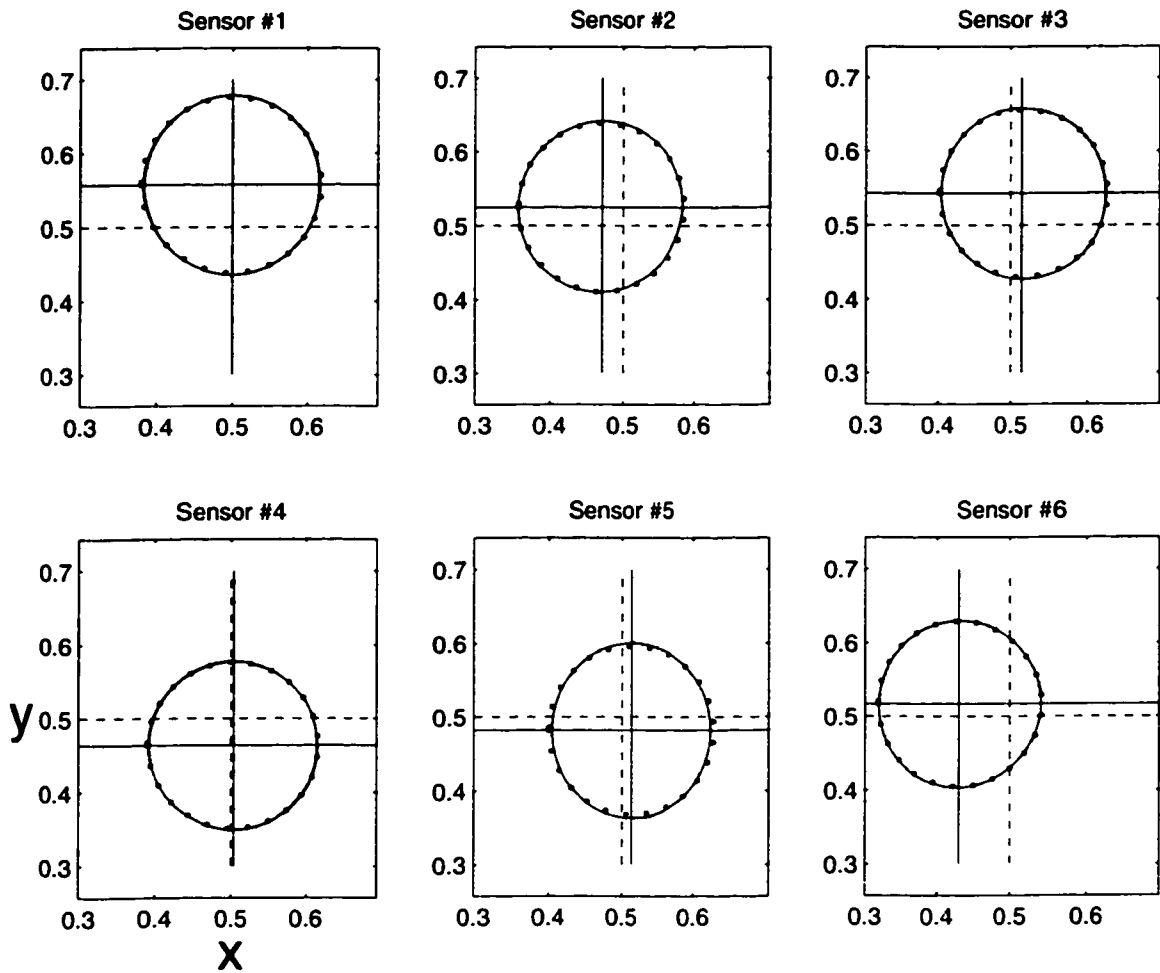


Figure 5.1: Plotted ratio centers

the X and Y values for each sensor through a full circle. The values plotted in Figure 5.1 are the raw ratios for each of the sensors. The dots indicate a perfect circle for an ideal sensor identically centered. The markers in dashed lines represent the expected values (from the specification sheet of the sensors) of the “center” of the sensors — at a ratio of 0.5 with an even spread of  $\pm 30\%$ . That is, the ratios should span 0.2 to 0.8. However, it is clear that each of the sensors were offset from this ideal; the translation of the crosshairs to reflect the true center of the data is indicated by solid crosshairs in each diagram. These centers  $X_{Offset}$  and  $Y_{Offset}$  are noted in Table 5.1, and were computed by taking the average of the X and Y values around the circle.

Consequently, to obtain from the raw ratios X and Y the corresponding angular



Sensor	$X_{Offset}$	$Y_{Offset}$
1	0.4999	0.5573
2	0.4716	0.5247
3	0.5152	0.5432
4	0.5036	0.4637
5	0.5141	0.4820
6	0.4296	0.5171

Table 5.1: Sensor centers

values, one must first correct it by subtracting the  $X_{Offset}$  and  $Y_{Offset}$  values. In the following, the corrected values are denoted by their lowercase equivalents; that is  $x = X - X_{Offset}$  and  $y = Y - Y_{Offset}$ .

### Step 1, Phase 2

The relationship between  $x, y$  data and angle are given by Figure 5.2. Using the corrected  $x, y$  data, theta and rho are computed as follows:

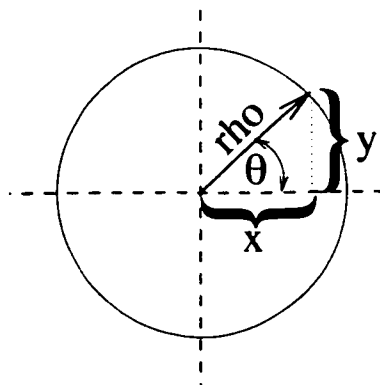


Figure 5.2: Theta and rho

$$\theta = \arctan\left(\frac{y}{x}\right) \quad \text{and} \quad \rho = \sqrt{x^2 + y^2}. \quad (5.1)$$

However, this angle  $\theta$  is not the same as the angle of the sensor relative to absolute vertical. (In fact, the sensors were deliberately rotated off-axis in response to error concerns in Section 3.5.)

Thus the second phase of the initial calibration was to compute the coordinate rotation necessary to align the sensors with the absolute vertical. This was accom-

plished by positioning the sensors on the fixed beam in each of four directions: up, out, down, and in. The resulting data provided the rotational correction necessary to establish the vertical direction and direction of rotation for each of the sensors.

Note the angle (in radians) of the absolute vertical for each of the sensors in Table 5.2; this is thus the angle  $\theta_{Offset}$  of rotation necessary to correct the computed  $\theta$  values to reflect “true” angles.

Sensor	$\theta_{Offset}$
1	84.1°
2	57.4°
3	49.2°
4	37.2°
5	46.9°
6	60.9°

Table 5.2: Sensor rotation calibration

### Step 1, Phase 3

Phase 3 of the initial calibration involved processing the data from phase 2 in MATLAB to provide an accurate direction comparison of subject data. The values plotted from within MATLAB are shown in Figure 5.3, and provide a representative sample of the four axes. The arrows shown in the six sensor plots represent the direction of up as the sensor is resting. The length and clustering of the four points was dependent on the amount of time spent in the position and the precision of the measures. The precision was measured as  $\pm 0.39^\circ$  during static conditions.

The noted eccentricity of the elliptical shape of the values shown in Figure 5.1 results in positioning error. This positioning error can be visualized in Figure 5.4 where the sensor is off axis with respect to the  $uv$  plane. See Section 5.1.1 below for a discussion of the cause and effect of this eccentricity error, it was determined that this error for each of the six sensors was negligible.

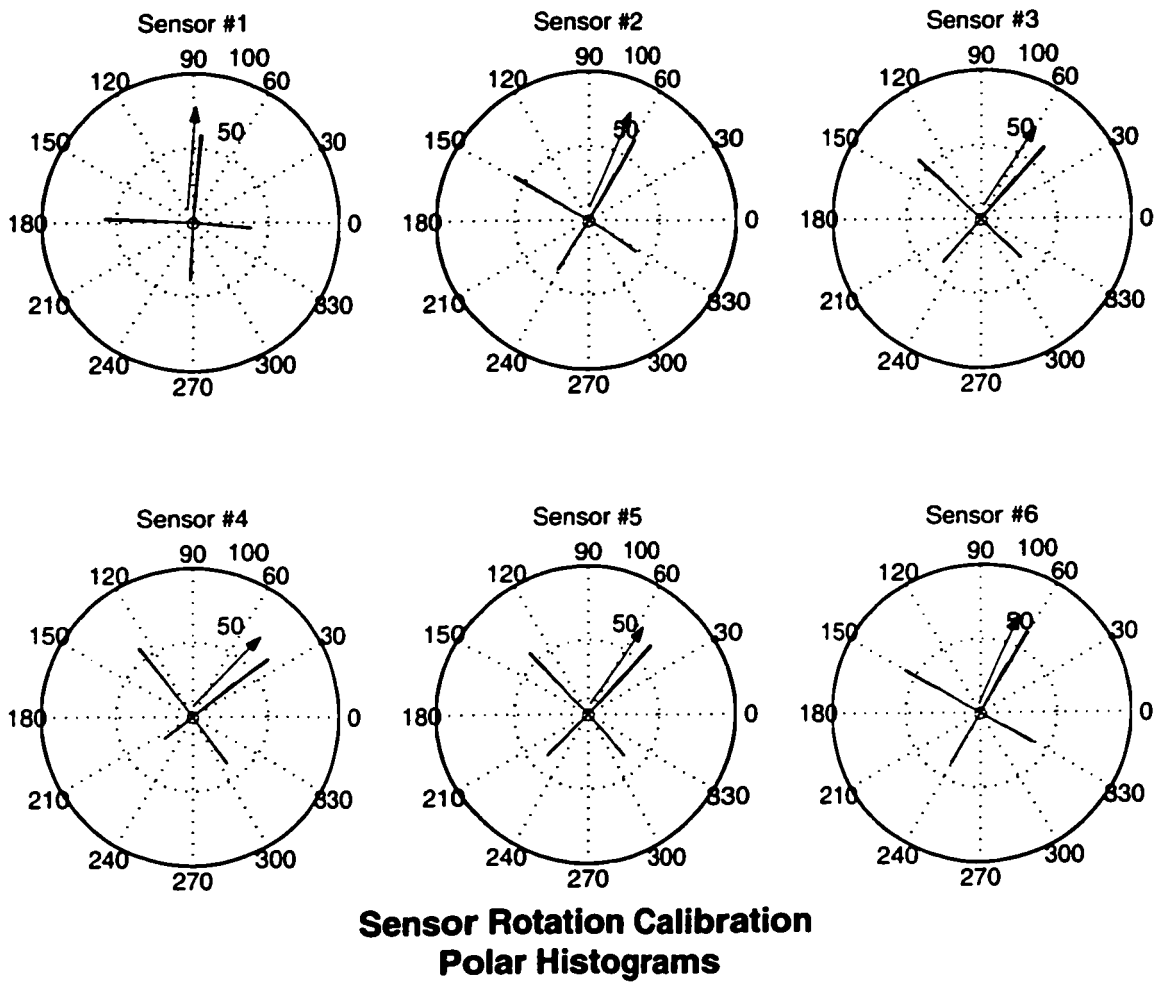


Figure 5.3: Polar histogram over 4 positions for the six sensors

## Step 2

The second step of the calibration, to be conducted by the subject at regular intervals, is a request for the subjects to assume a specific posture. This posture should be a “perfect” one which allows an accurate comparison to be made with the subject’s more typical (and perhaps poor) posture. For example, this posture could be an upright back-against-the-wall posture, either standing or sitting. This position should be held for a 5 min period at least once every 4 hours, for example, to prevent artifacts of analysis arising from any gradual shifting or movement of the sensors on the subject’s spine. Thus, this data were used to assure the positioning of the sensors on the back.

An example of rigid back data can be seen in Figure 5.15.

### 5.1.1 Error Correction

The sensors give data which allows the accurate computation of angles in one plane. However, these sensors may be rotated, either in the process of constructing the sensor assemblies, or when placed on a subject’s spine, such that their plane of measure is at an angle with the sagittal plane. In this case, a 360° circle would instead have the appearance of an ellipse, as it is projected from the measured plane onto the sagittal plane. This in turn introduces an error in the angle measured using equation (5.1).

This error can be characterized in two ways.

Firstly, suppose the sensor is rotated in the frontal plane. Then off-axis angles will be either under- or over-estimated. To see this, let our coordinate system be denoted  $(u, v, w)$ , with  $u$  the direction perpendicular to the spine in the sagittal plane,  $v$  the vertical, and  $w$  the remaining orthogonal direction in the frontal plane. (This is done to avoid confusion with  $x$  and  $y$  above, which are rotated in the  $uv$  plane.)

Then a rotation through angle  $\phi$  in the  $vw$  plane is given by multiplying these coordinates by the matrix

$$R_{\phi} = \begin{bmatrix} 1 & 0 & 0 \\ 0 & \cos \phi & -\sin \phi \\ 0 & \sin \phi & \cos \phi \end{bmatrix}.$$

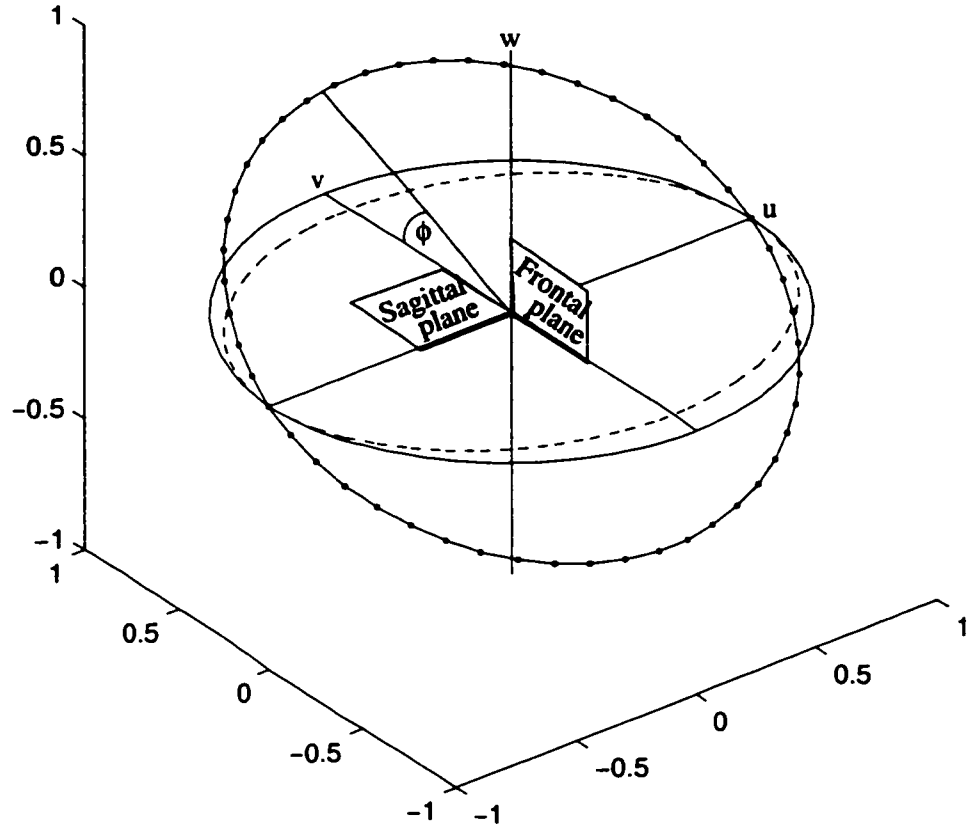


Figure 5.4: Error with projected error

The sensor measures a circle in the image of the  $uv$  plane under  $R_\phi$ ; but it is necessary to determine the angle of rotation in the actual  $uv$  plane. This is equivalent to applying an orthogonal projection back to the  $uv$  plane:

$$P = \begin{bmatrix} 1 & 0 & 0 \\ 0 & 1 & 0 \\ 0 & 0 & 0 \end{bmatrix}.$$

An example of the projected elliptical shape is shown in Figure 5.4. The solid line circle in Figure 5.4 represents the ideal sensor in the sagittal plane. The dotted line circle represents the a sensor with a rotation  $\phi$  of  $30^\circ$ . The dashed line circle is the projection of the tilted sensor to an elliptical shape into the sagittal plane.

The composition  $P \circ R_\phi$  takes  $(u, v)$  to  $(u, v')$ , where  $v' = \cos(\phi)v$ . Table 5.3 compares the (correct angle)  $\arctan(v/u)$  with the (measured angle)  $\arctan(v'/u)$ , for various values of rotation  $\phi$ . It follows that a rotation of up to  $10^\circ$  produces no more

$$\phi = 5^\circ$$


---


$$\cos(5^\circ) = 0.9962$$

at 30°	29.91°
at 45°	44.89°
at 60°	59.91°

$$\phi = 10^\circ$$


---


$$\cos(10^\circ) = 0.9848$$

at 30°	29.62°
at 45°	44.56°
at 60°	59.62°

$$\phi = 30^\circ$$


---


$$\cos(30^\circ) = 0.866$$

at 30°	26.57°
at 45°	40.56°
at 60°	56.31°

Table 5.3: Sensor Positioning Error

than a  $0.5^\circ$  error in the angle measured. For larger angles, the error in measurement is more significant; but on the other hand, larger angles are easily visible to an observer. If an estimate of the angle of error  $\phi$  is generated (for example, by taking a photograph of the subject's back with sensors in place), then data can be corrected by scaling  $v$  by the factor  $\frac{1}{\cos \phi}$  prior to applying equation 5.1.

Secondly, consider the case (as in Phase 3 of the initial calibration) where a plot of the full  $360^\circ$  of the sensor is available. If there is a sensor positioning error, the resulting plot will be elliptical in shape, resulting in a similar distortion of the angular data. In this case, however, there are two options for correcting the data.

The first option is to draw up a table of angles based on the absolute position of the sensor at each step (of the stepper motor, for example), and interpolate within that set to deduce the correct angle in the vertical plane from the measured angle in the plane of the sensor assembly. This is straightforward, but now the accuracy of the measured angle is a function of the accuracy (and repeatability) of the angles of

the steps of the stepper motor.

The second option is to carry out a mathematical correction, as above. This time, however, the angle  $\phi$  of rotation out of plane is unknown, so a different method to calculate the necessary scaling. Assume for simplicity that the ellipse is aligned with the axes, so that the corresponding equation for the ellipse is simply of the form

$$x^2 + (cy)^2 = r^2, \quad (5.2)$$

for some  $c \neq 1$ . The value  $c$  is computed by substituting data points (or averaged data points) into equation (5.2). If the data for  $y$  is scaled by a factor of  $c$  (giving  $y' = cy$ ) then the equation (5.1) will return the true value of the angle  $\theta$ .

In this section the values of rho, the length of the vector observed have been ignored, but note that they, too, contain information as to the sensor positioning error. In the direction of the vertical there is a constant vector of length corresponding to one gravity; the observed vector will become shorter as the sensor rotates away from the vertical.

## 5.2 Analysis

In this section the analysis of actual data obtained from a subject's spine through various activities is discussed. The sensors were affixed to the subject's spine using medical bandage tape to secure the sensors to the skin. Sensor placement is indicated in Figure 5.5 (adapted from [13]). The attached wires were also taped, but with additional play to prevent the drag of the wiring from damping the sensors' response. The cable was left long enough as to allow the data logger to be tucked into a shirt or pants pocket.

Two types of data were collected. In the first case, the subject assumed a series of twelve postures, holding each for a 5 minute period. In the second case, nonregimented data were collected while day-to-day activities took place. All data were sampled in 15 second epochs and saved in 10-minute files.

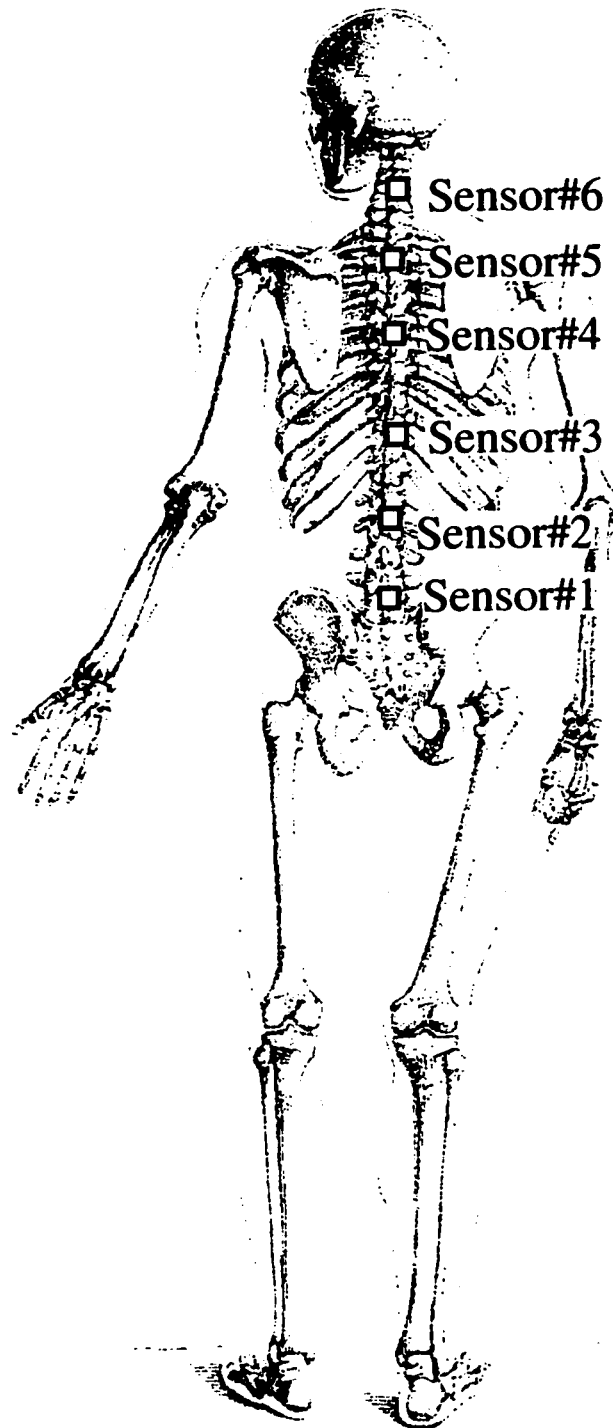


Figure 5.5: Sensor locations



The collected data was concatenated and then processed in blocks. It was parsed for sensor dropout and checksum failure and also converted to a MATLAB-readable form using a postprocessing program, as described earlier.

The analysis program took the incoming data (in the form of average  $T1$  and  $T2$  periods), and created vectors of ratios for each of X and Y. This data was then centered by removing the Offsets described in the previous section, yielding corrected data  $x$  and  $y$ . These values were then converted to polar coordinates using equation (5.1), and finally rotated to give true angles relative to vertical using the offset values of Table 5.2.

### 5.2.1 Regimented Posture Data

To understand the data from the regimented posture phase better, stick figures were developed to model the subject's movement. The stick figures represent a first derivative approximation of each of the sensors (corrected) angles joined at a unit difference. Perpendicular lines of a half unit demonstrate the change of angle. In other words, the figures are drawn as a stack of  $\perp$  shapes, each at the sensor's corrected angle. The "dot" at the top of the figures represents the subject's head and is at the same angle as the sixth sensor. The line segments, from bottom to top, are sensors #1 through #6.

The twelve postures associated with the figures on the following pages are detailed in Table 5.4.

- (A) Figure 5.6 Standing with Back Against Wall. This is the first in the series of twelve series of postures. It is an upright posture where the subject's buttocks and shoulder blades are flat against the wall.
- (B) Figure 5.7 Sitting in a Chair: back against the rear of the chair.
- (C) Figure 5.8 Sitting Slouched Forward: subject was facing and hunched over the rear of the chair
- (D) Figure 5.9 Prostrate on Table: face down, back flat, feet angled off to rest on the floor
- (E) Figure 5.10 Touching Toes: subject was bent forwards as if touching toes
- (F) Figure 5.11 Recline Head on Pillow: subject was flat on their back with their head on a pillow
- (G) Figure 5.12 Recline Face Down: subject was laying face down, with no pillow
- (H) Figure 5.13 Rocking Chair1: rocking in a rocking chair, 2 second cycle of 12cm swing
- (I) Figure 5.14 Rocking Chair2: sitting in a rocking chair with no movement
- (J) Figure 5.15 Sitting with Back Against the Wall: attempting to sit with the back as straight as possible.
- (K) Figure 5.16 Slouch Head Back: slouching with head as far back as possible
- (L) Figure 5.17 Up Down Stairs: walking continuously up an down a flight of 12 steps, 5-7 seconds for every ascension and decent

Table 5.4: Twelve regimented postures

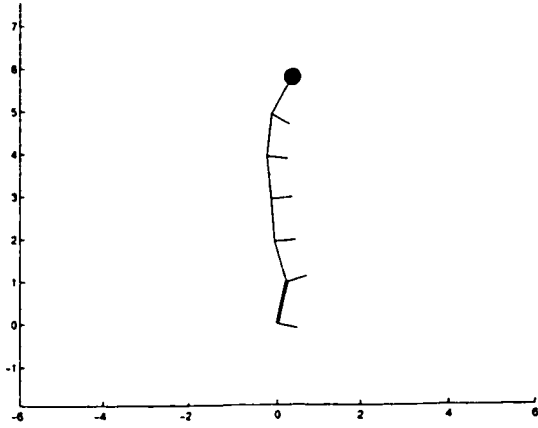


Figure 5.6: Standing with Back Against Wall

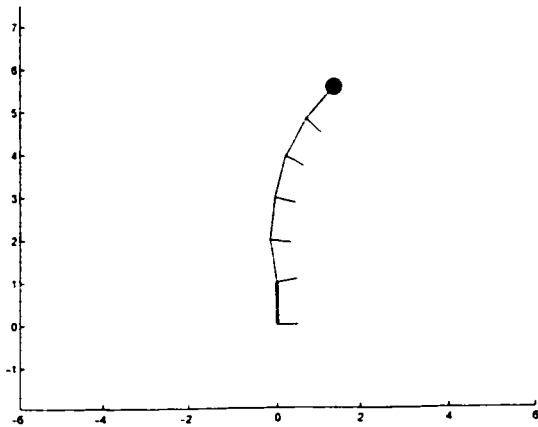


Figure 5.7: Sitting in a Chair

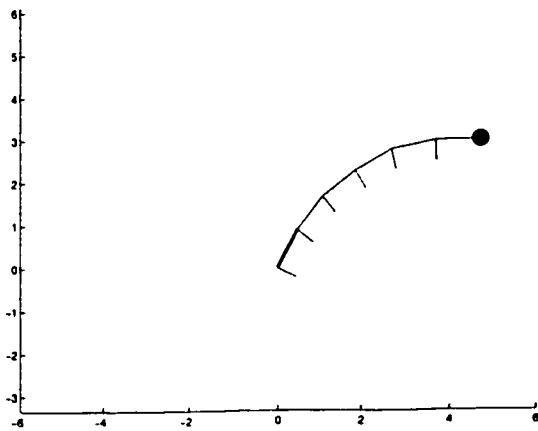


Figure 5.8: Sitting Slouched Forward

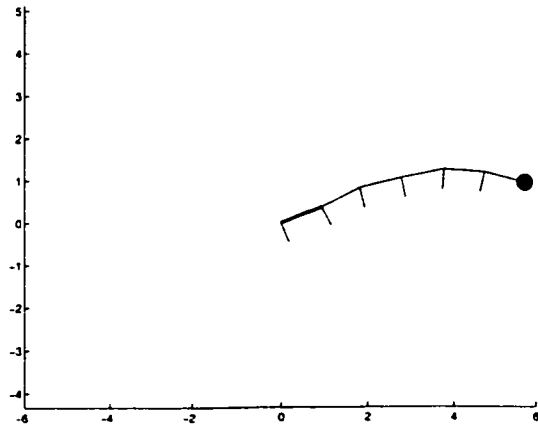


Figure 5.9: Prostrate on Table

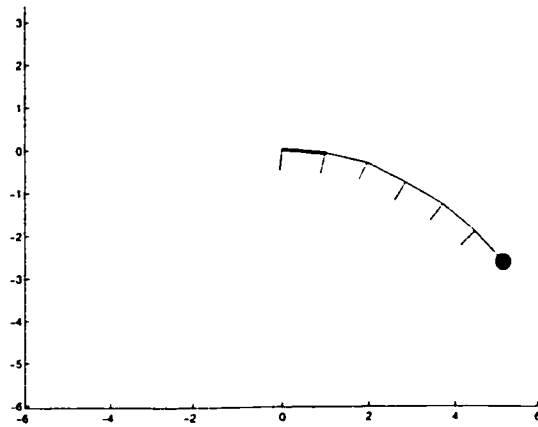


Figure 5.10: Touching Toes

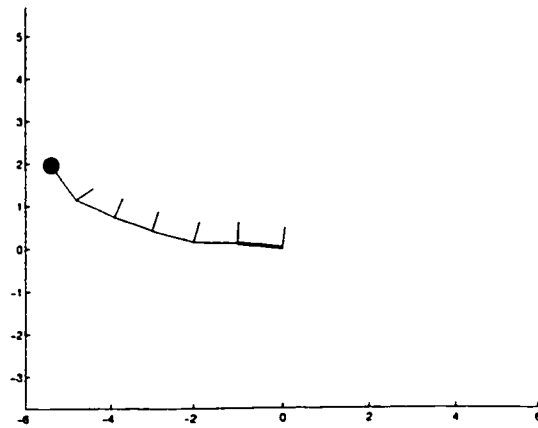


Figure 5.11: Recline Head On Pillow

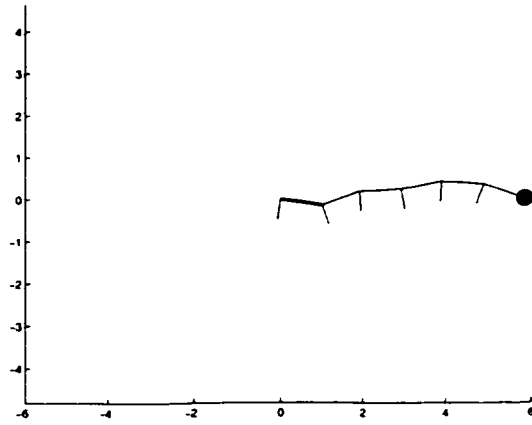


Figure 5.12: Recline Face Down

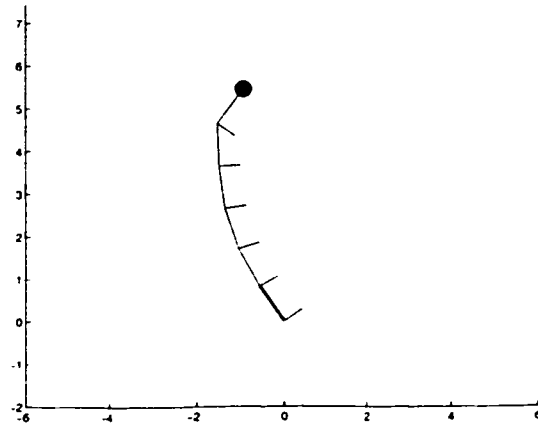


Figure 5.13: Rocking Chair1

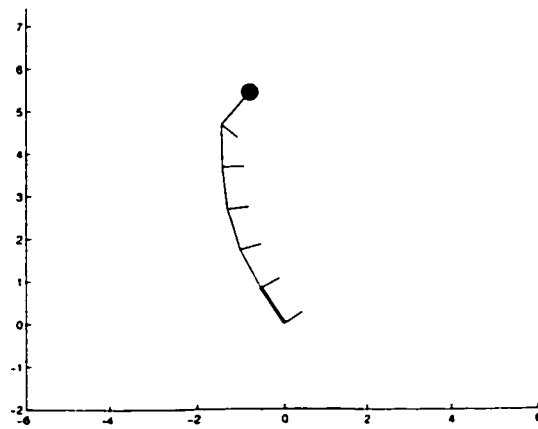


Figure 5.14: Rocking Chair2

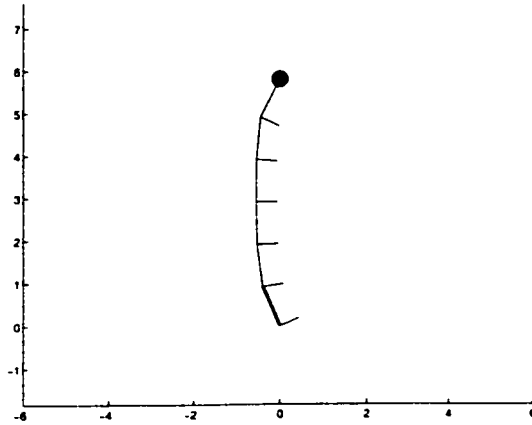


Figure 5.15: Sitting with Back Against the Wall

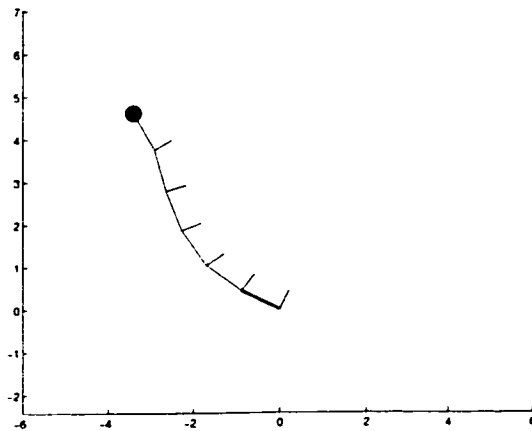


Figure 5.16: Slouch Head Back

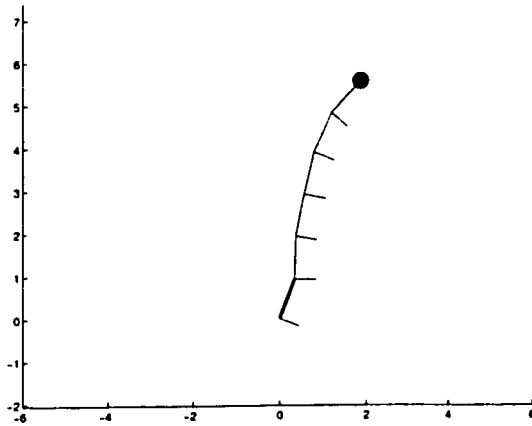


Figure 5.17: Walking Up Down Stairs

The broader view of the twelve regimented steps over the course of an hour is shown in Figure 5.18. The epochs are 15 second. The sensor angle, is the corrected sensor angle that is in the  $u - v$  plane. Each of the twelve postures the subject was requested to remain motionless for 5 minutes (unless there was a motion task involved). The flat segments are each 5 minutes long, indicating where the subject held the postures. The postures are associated with the letters (A-L) listed in Table 5.4. The spikes between the flat areas correspond to the subject changing position. In columns (H) and (L) - corresponding to rocking and climbing stairs - the movement is averaged out. (Slight movement is visible when viewing an animated sequence of the regimented postures.) Figure 5.19 shows standard deviation of the raw sensor timing counts for uncorrected  $X$  and  $Y$  for all accelerometers. The standard deviation is calculated by the whole-score method. The whole-score method is derived by:

$$\begin{aligned}
 S &= \sqrt{\frac{\sum(x^2)}{N}} \implies S^2 = \frac{\sum(X - \bar{X})^2}{N} \\
 S^2 &= \frac{(\sum X^2 - 2\bar{X} \sum X + N\bar{X}^2)}{N} \\
 S^2 &= \frac{\sum X^2}{N} - 2\bar{X} + \bar{X}^2 \\
 S &= \sqrt{\frac{\sum X^2}{N} - \bar{X}^2} \implies S = \frac{\sqrt{(N \sum(X^2)) - (\sum X)^2}}{N}
 \end{aligned}$$

Population standard deviation is used to simplify the calculations and the variance  $\frac{N}{N-1}$  was deemed to be small enough to ignore for the large  $N$ 's involved.

Note the increases in columns (H) and (L), where the motion artifact is averaged out of the data, but is apparent in the standard deviations. The variations of sensor #6 (at the neck), are due to the subject talking and interacting with the environment while rocking, and looking up while ascending and descending the stairs.

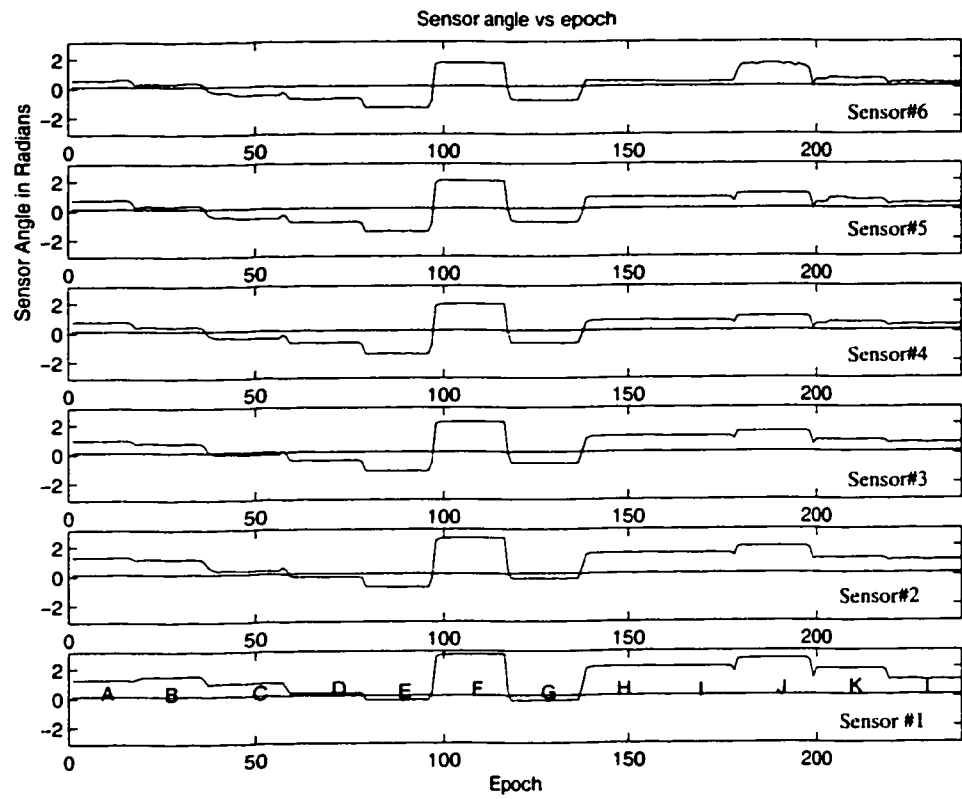


Figure 5.18: Twelve posture positions over a one hour period of regimented postures



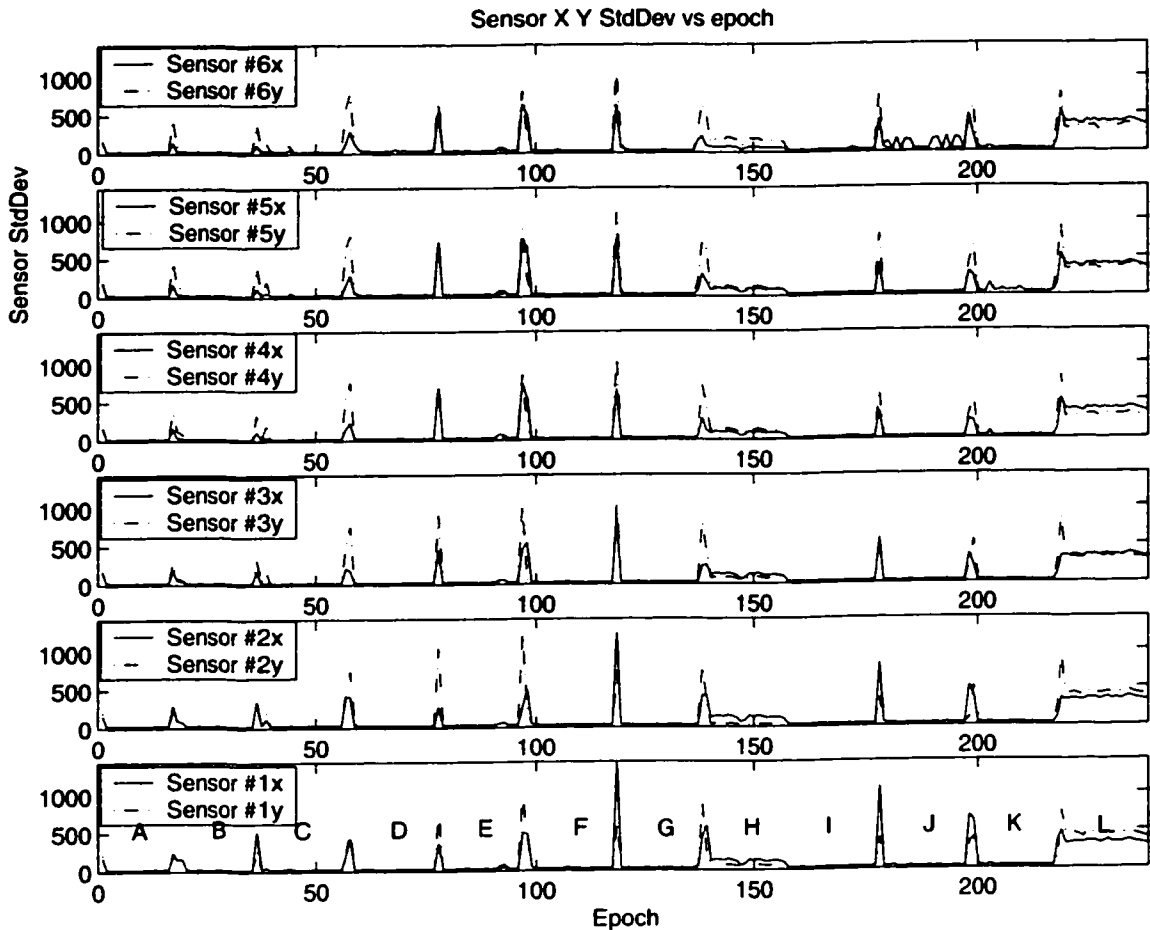


Figure 5.19: Standard deviation over a one hour period of regimented postures

### 5.2.2 Unregimented data

In Figure 5.20 the subject was attached to sensors over a five hour period in the evening. The first hour, up to 240 epochs, was spent doing household duties and activities, the following four hours was doing desk work sitting in an office chair. The period can be broken down into:

- (a) playing with child;
- (b) chatting with spouse;
- (c) preparing a meal;
- (e) eating;

- (f)** dishes and cleanup;
- (g)** a 5 min snooze on the couch;
- (h)** preparation for evening work;
- (j)** desk work, mostly typing;
- (k)** head back semi-reclined;
- (l)** washroom; then returning to desk work.

All epochs are 15 seconds long. The raw count standard deviations of X and Y sensors are shown in Figure 5.22; note the large movements in while the subject conducted household chores and minimal movement later in the evening. The spikes and peaks from (h) to the end of the trial represent posture shifts: leaning forward, backward, with occasional stretches.

Histograms of the corrected sensor angle (see Figure 5.21), show very little change over the course of the 5 hours. The histograms are the total count of the angles in one degree bins. The clustering of these angles is an indication of how much time is spent at those angles and thus those postures. A more easily interpreted manner of displaying this data is in the form of an animation of the “stick figure”, with a frame corresponding to each epoch. This allows the possibility to pinpoint the time periods during which the subjects posture was both good and less that ideal.

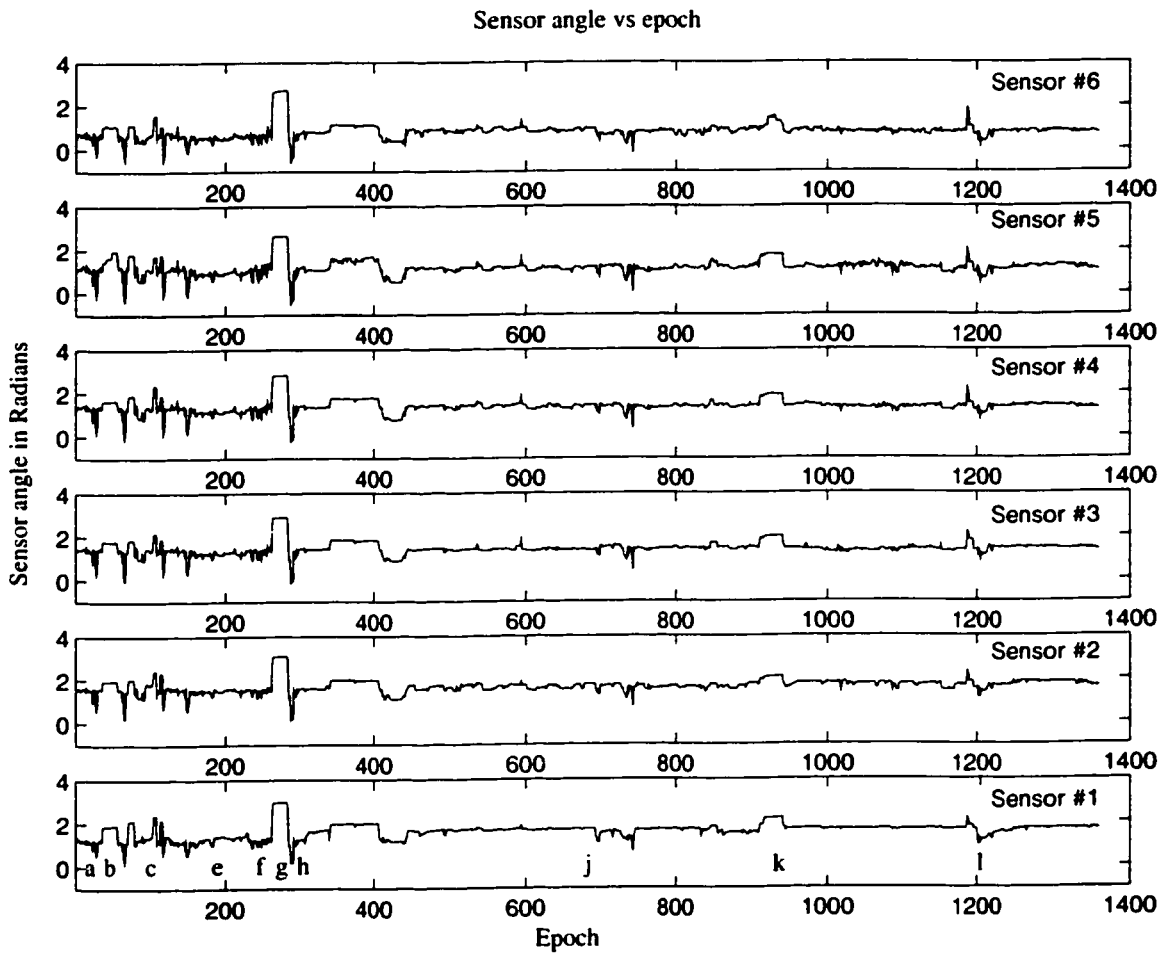


Figure 5.20: Spine angles over a five hour period

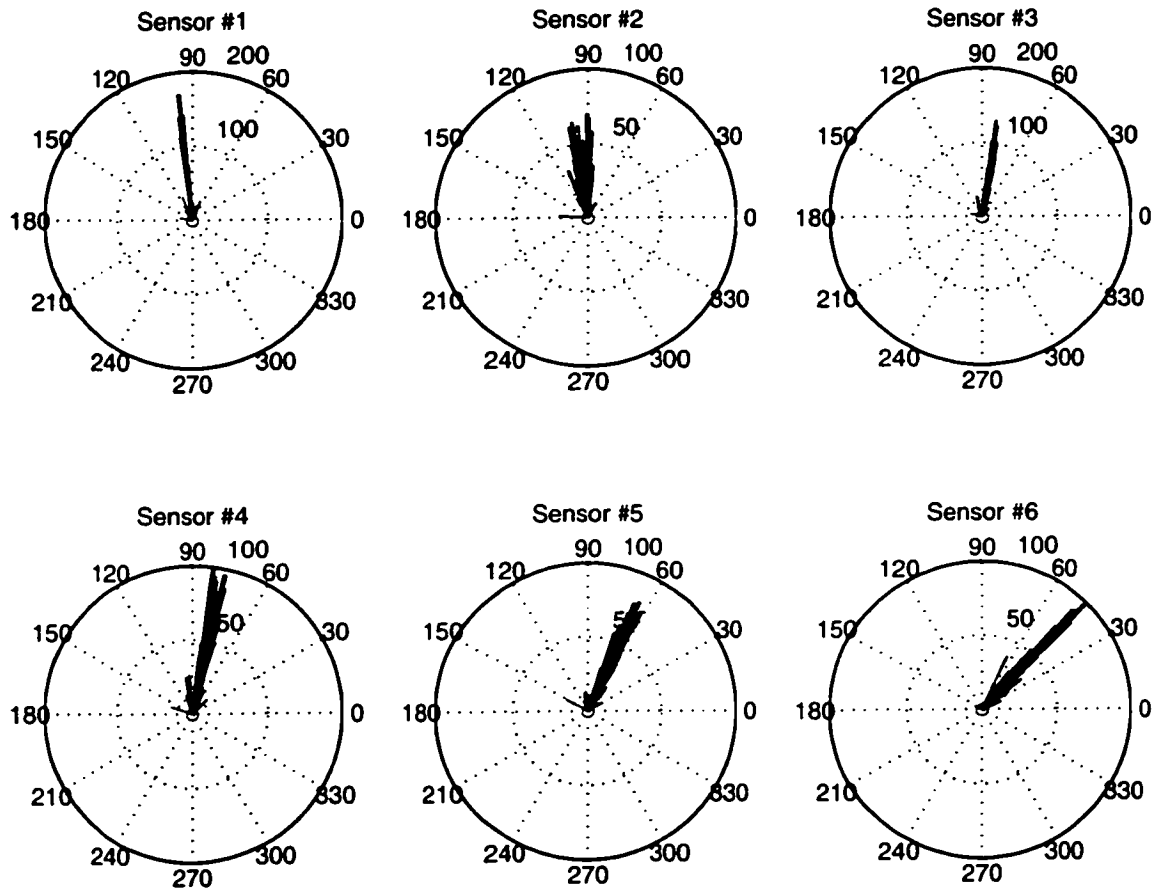


Figure 5.21: Histograms of the corrected sensor angle over a five hour period

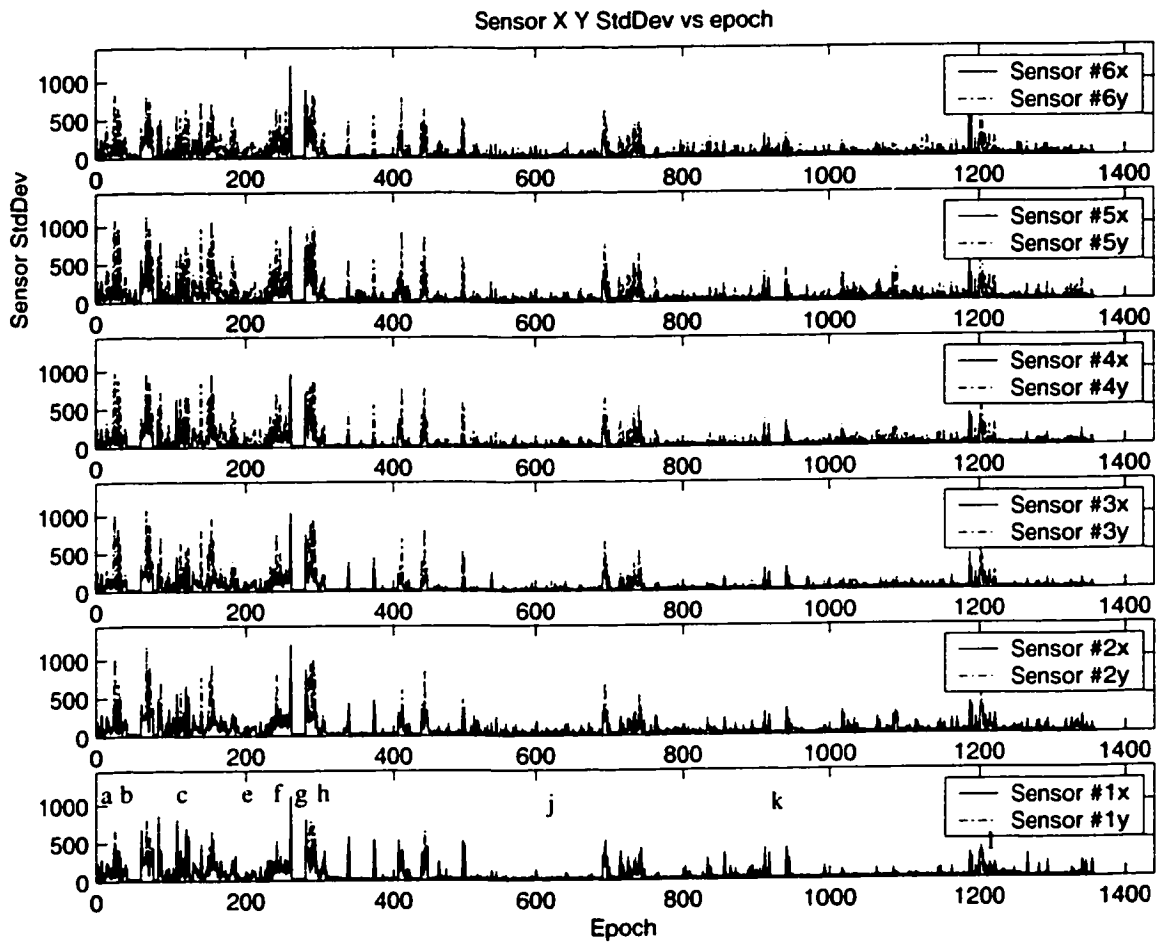


Figure 5.22: Raw count standard deviations of X and Y sensors over a five hour period

# Chapter 6

## Conclusions and Suggestions for Future Work

### 6.1 Conclusion

The primary issue examined in this research was the idea that traditional posture related studies looking at short term locomotion failed to determine overall sagittal plane angles of the spine. There were two objectives set forth at the beginning of this research:

*Objective #1* To develop/create a facilitator for a long term study of posture, which may also be used to examine aspects of idiopathic scoliosis. This includes creating a multiuse, low power, low cost and easy to use data logger.

*Objective #2* To examine low frequency use of accelerometers to monitor spinal inclinations in the sagittal plane.

Both of these objectives were met. As results of the studies conducted, it can be concluded that utilizing over-sampled accelerometer readings spinal posture in the sagittal plane can be monitored. Using the developed posture measuring device, long term data can be collected during activities of daily living.

Further research involving multiple subjects and clinical trials could validate long term correlation of subject posture.

In practice once the data had been collected, an experimenter or technician can run the data through a streamlined version of the analysis of Section 5.2. As was

done for the unregimented data in this study, small animations of the collected data can be made to explain the data in a simplified form. This could also be used to demonstrate correct or pinpoint poor posture to the subject. A further augmentation could be that displayed collected data with a natural form (rather than a stick figure).

The overall low cost of use and reuse by a subject makes this device available for longer term studies over days to months; its efficient design makes this a feasible prospect.

To use the posture measurement system for longer studies involving thousands of files or for more intense data collection than presented here, some modifications would be needed. One such modification is to the file system. The file system should use sub-directories to separate multiple runs of data. This would allow for a greater number of files to be written.

If continuous recording is not desired, various aspects of the system could be modified to take advantage of the corresponding “down-time”. The sensors could be powered down between sample times. (This would entail ramp up times of one to two cycles of  $T_2$  to stabilize measures prior to collection data.) Sleep modes in the satellite processors and the master processor could be modified to take advantage of a sleep/shutdown mode that requires less than  $1\mu A$ . An external wake timer could be used in such an instance. This could potentially allow the data logger to last weeks on a single set of batteries.

# Chapter 7

## Afterword (or if I had to do this again...)

One enhancement that would have been extremely useful would have been a SPI to serial interface for the debugging/programming user interface I/O (I.E. MAX3100 or MAX3310). This would have provided a secondary debugging interface so debugging would not interfere with with inter-processor communications.

The ATmega103L is spec'ed at up to 3.7 volts but is tolerant for short periods for in-circuit serial programming (ISP). The ATMEL documentation does not reflect this information although it is used in the SK300 demo board. Two circuit methods of programming can be used: the one used in the core module directly connects the ISP to the board; the other common method is to gate external accesses (I.E. external RS232 buses) through a multiplexer. In retrospect this would have been a better choice, as the disruption of switching out the debugging terminals during each programming session was time consuming.

Ordering the compact flash connector prior to seeing the full data sheet was short sighted. Although functionally not important, it would have been aesthetically pleasing to have the CF card facing "up" rather than facing down thus hidden from view.

It would have been advisable to have obtained the case and sensor connectors in advance. If the case was obtained or minimally spec'ed out there would have been no need to "carve" the board to fit. As it was the case was chosen based on the rough outline of the assembled boards and guessed sizes of the facilities for user interface.



If the sensor connectors were chosen prior or during the design phase less time would have been needed to adapt and modify the connectors. Over the course of the study the sensors were wired up in 5 separate variations, which may have put undue stress upon the sensor assemblies.

No doubt utilizing the Compact Flash would have been more convenient if the 8 bit file system was available. It would have reduced code space and creation time, although at the cost of compatibility with other devices or power.

LCD monitors would have made more information available to the subject. A menu system could have been devised to take advantage of an LCD. While researching parts for the user interface it became apparent, however, that there are few, if any, LCDs that run at 3.3V and that are commercially available in small quantities. This hampered any local display on the data logger.

To allow easy prototyping, DIP-20 chips were used — if it was to be redesigned SMT devices would have been chosen. By utilizing SMT devices the overall structure could have been smaller and the overall cost reduced. In-circuit programming could have been managed through switches or jumpers.

Further investigation into matching standard deviation data and subject movement would be an interesting direction to attempt. The use of neural-net, genetic programming or other learning type of software to characterize the data or minimally group and bin the data. A serious look at mounting the sensors on the subjects will have to be done, the method used was uncomfortable.

# Bibliography

- [1] Analog Devices, Inc. *Low Cost 2g Dual-Axis Accelerometer with Duty cycle outputs*, 2000.
- [2] Atmel Corporation. *AVR RISC Microcontroller Data Book*, 1999.
- [3] AVR-Forum. <http://www.avr-forum.com/avrsource.html>, 2001.
- [4] O. Baltag, D. Costandahe, and Salceanu A. Tilt measurement sensor. *Sensors & Actuators A-Physical*, 81:336-9, 2000.
- [5] C.T.M. Baten, P. Oosterhoff, I. Kingma, P.H. Veltink, and H.J. Hermens. Inertial sensing in ambulatory back load estimation. In *Engineering in Medicine and Biology Society, 1996. Bridging Disciplines for Biomedicine., 18th Annual International Conference of the IEEE*, volume 2, pages 497 - 498, 1996.
- [6] C.V.C. Bouten, K.T.M. Koekkoek, M. Verduin, R. Kodde, and J.D. Janssen. A triaxial accelerometer and portable data processing unit for the assessment of daily physical activity. *Biomedical Engineering, IEEE Transactions on*, pages 136 - 147, 1997.
- [7] M. Bramanti and A. Tozzi. New method for motion measurement and control. *Journal of BioMedical Engineering*, 12(5):451-2, 1990.
- [8] J.R. Cobb. Outline for the study of scoliosis. *Am. Acad Othop.*, 5:261-275, 1948.
- [9] CompactFlash Association. *CF+ and CompactFlash Specification Revision 1.4*, 1999.
- [10] Dave Dunfield. *Mdcfs: Minimal dos compatible file system*, 1993.
- [11] F Foerster, M Smeja, and J. Fahrenberg. Detection of posture and motion by accelerometry: a validation study in ambulatory monitoring. *Computers in Human Behavior*, pages 571-583, 1999.
- [12] M. Halioua, T.S. Liu, H.C. and Bowins, and J.K Shih. Automated topography of human forms by phase-measuring profilometry. In *Surface Topography and Spinal Deformity VI*, pages 6-16, 1992.
- [13] J. Harter, editor. *Images Of Medicine*. Bonanza Books, 1991.
- [14] A Heyn, RE Mayagoitia, AV Nene, and PH Veltink. The kinematics of the swing phase obtained from accelerometer and gyroscope measurements. In *Proceedings of the 18th Annual International Conference of the IEEE Engineering in Medicine and Biology Society. 'Bridging Disciplines for Biomedicine'*, pages 463-4, 1996.

- [15] E. Hierholzer and B. Drerop. Three-dimensional reconstruction of the spinal midline from rastersteriographs. In *Surface Topography and Spinal Deformity V*, pages 53–55, 1990.
- [16] Seth Hollar. Cots dust. Master's thesis, University of California, Berkeley, 2000.
- [17] VI Kadushkin, FZ Rozenfel'd, and VF Udalov. Contactless magnetic diode displacement sensor. *Measurement Techniques*, pages 339–40, 1987.
- [18] Satoshi Kurata, Masaaki Makikawa, Hideteru Kobayashi, Ayumu Takahasahi, and Rinzo Tokue. Joint motion monitoring by accelerometers set at both near sides around the joint. In *Proceedings of the 20th Annual International Conference of the IEEE Engineering in Medicine and Biology Society.*, volume 20, pages 1936–9, 1998.
- [19] Zvi Ladin and Ge Wu. Combining position and acceleration measurements for joint force estimation. *Journal of Biomechanics*, 24:1173–1187, 1991.
- [20] Altium Limited. Protel 99, 1999.
- [21] J C Lotters, J Schipper, P H Veltink, W Olthuis, and P. Bergveld. Procedure for in-use calibration of triaxial accelerometers in medical applications. *Sensors & Actuators A-Physical*, 68:221–228, 1998.
- [22] Edmond Lou. *An Electromagnetic Approach to the Treatment of Scoliosis*. PhD thesis, University of Alberta, 1998.
- [23] HJ Luinge, PH Veltink, and CTM Baten. Estimating orientation with gyroscopes and accelerometers. *Technology & Health Care*, pages 455–9, 1999.
- [24] Lafortune M.A. Three-dimensional acceleration of the tibia during walking and running. *Journal of Biomechanics*, pages 877–886, 1991.
- [25] RE Mayagoitia, SCM Dutson, and BW Heller. Evaluation of balance during activities of daily living. In *Proceedings of the First Joint BMES/EMBS Conference. 1999 IEEE Engineering in Medicine and Biology 21st Annual Conference and the 1999 Annual Fall Meeting of the Biomedical Engineering Society*, page 520, 1999.
- [26] R.E. Mayagoitia, J.C. Lotters, and P.H. Veltink. Standing stability evaluation using a triaxial accelerometer. In *Engineering in Medicine and Biology Society, 1996. Bridging Disciplines for Biomedicine., 18th Annual International Conference of the IEEE*, pages 573 – 574, 1997.
- [27] Microsoft Corporation. *Detailed Explanation of Fat Boot Sector*, 2000.
- [28] Microsoft Corporation. *FAT: General Overview of On-disk Format*, 2000.
- [29] J.R.W. Morris. Accelerometry – a technique for the measurement of human body movement. *Journal of Biomechanics*, pages 729–736, 1973.
- [30] A.K. Nakahara, Sableman E.E., and Jaffe D. L. Development of a second generation wearable accelerometric motion analysis system. In *Proceedings of the First Joint BMES/EMBS Conference. 1999 IEEE Engineering in Medicine and Biology 21st Annual Conference and the 1999 Annual Fall Meeting of the Biomedical Engineering Society*, volume 20, page 630, 1999.

- [31] G. Neugebauer, H. and Windischbauer. Effects of rotating the patient on moire contourgrams and verification of derotation in scoliosis by moire contourgrams. In *Moire Fringe Topography and Spinal Deformity*, pages 201-205, 1981.
- [32] R Roduit, P-A Besse, and J-P Micallef. Flexible angular sensor and biomechanical application. *IEEE Transactions on Instrumentation & Measurement*, pages 1020-2, 1998.
- [33] Scoliosis Research Society. <http://srs.org/htm/glossary/medterms.htm>, 2000.
- [34] Scoliosis Research Society. <http://srs.org/htm/review/review06.htm>, 2000.
- [35] Paul Stoffregen. <http://www.pjrc.com/tech/8051/ide/>, 2000.
- [36] I. Stokes. 3-d spinal deformity measurement methods and terminology. In *Int. Symposium on 3-D Scoliotic Deformities*, pages 236-243, 1992.
- [37] Stilson T. <http://www-ccrma.stanford.edu/ccrma/courses/252/sensors/node9.html>, 1996.
- [38] T13, Technical Committee,Maxtor Corporation. *Information Technology -AT Attachment with Packet Interface Extension (ATA/ATAPI-4)*, 1998.
- [39] T13 Technical Committee,Maxtor Corporation. *Information Technology - AT Attachment with Packet Interface - 5*, 2000.
- [40] Toko Corporation. *TOKO Data Book*, 2000.
- [41] A.R. Turner-Smith. A television/computer three-dimensional surface shape measurement system. *J. Biomechanics*, 21:515-529, 1988.
- [42] Eus J W Van Someren. Actigraphic monitoring of movement and rest-activity rhythms in aging, alzheimer's disease and parkinson's disease. In *Annual International Conference of the IEEE Engineering in Medicine and Biology - Proceedings*, pages 69-70, 1996.
- [43] P. Veltink, D. Nieuwland, J. Harlaar, and C. Baten. Inertial sensing in a hand held dynamometer. In *18th International Conference of the IEEE Engineering in Medicine and Biology Society*, pages 502-503, 1996.
- [44] P.H. Veltink, HansB.J. Bussmann, W. de Vries, WimL.J. Martens, and R.C. Van Lummel. Detection of static and dynamic activities using uniaxial accelerometers. *Rehabilitation Engineering, IEEE Transactions on*, pages 375 - 385, 1996.
- [45] P.H. Veltink, E.G.O. Engberink, B.J. Van Hilten, R. Dunnewold, and C. Jacobi. Towards a new method for kinematic quantification of bradykinesia in patients with parkinson's disease using triaxial accelerometry. In *Engineering in Medicine and Biology Society, 1995., IEEE 17th Annual Conference*, pages 1303 - 1304, 1995.
- [46] P.H. Veltink and H.M. Franken. Detection of knee unlock during stance by accelerometry. *Rehabilitation Engineering, IEEE Transactions on*, pages 395 - 402, 1996.

- [47] Jan H Waarsing, Ruth E Maygoitia, and Peter H. Veltink. Quantifying the stability of walking using accelerometers. In *Annual International Conference of the IEEE Engineering in Medicine and Biology - Proceedings*, pages 469–470, 1996.
- [48] Harvey Weinberg. *Using The ADXL202 Duty Cycle Output*. Analog Devices, Inc., 1998.
- [49] A. Willemsen, F. Bloemhof, and H. Boom. Automatic stance-swing phase detection from accelerometer data for peroneal nerve stimulation. *Biomedical Engineering, IEEE Transactions*, pages 1201–1208, 1990.
- [50] A. Willemsen, J.A. van Alste, and H.B.K. Boom. Real-time gait assessment utilizing a new way of accelerometry. *Journal of Biomechanics*, pages 859–863, 1990.
- [51] Ge Wu and Zvi Ladin. The kinematmeter - an integrated kinematic sensor for kinesiological measurements. *Journal of Biomechanical Engineering*, 115:53–62, 1993.
- [52] Ge Wu and Zvi Ladin. The study of kinematic transients in locomotion using the integrated kinematic sensor. *Rehabilitation Engineering, IEEE Transactions on*, 4:193 – 200, 1996.
- [53] X3T10 Technical Committee, Maxtor Corporation. *Information technology - AT Attachment Interface with Extensions (ATA-2)*, 1994.

# Appendix A

## Master Schematic

The schematic for the master processor and the Compact Flash connector is given in Figure A.1. It and the satellite board were designed using Protel. Note that it is a two-sided board, with the processor on the bottom and the Compact Flash on the top; this design made the most efficient possible use of space.

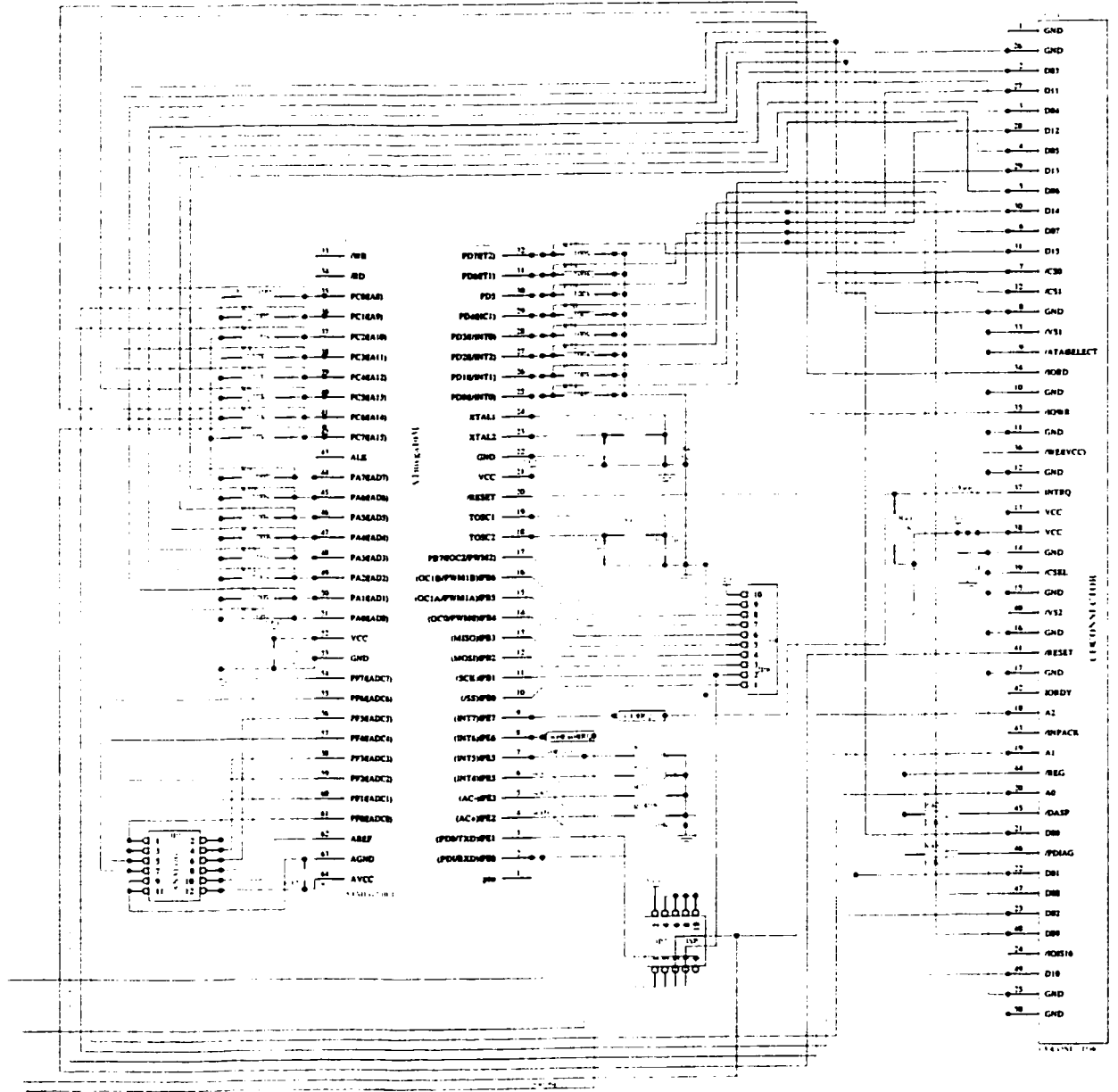


Figure A.1: Schematic of the Master processor and CF connector

# Appendix B

## Satellite Schematic

The schematic for the satellite board with its six satellite processors is given in Figure B.1. The headers (at the top of the diagram) were used exclusively for debugging purposes and have no connections at run time. The header seen on the left side, one third of the way up the diagram, is the connection for the accelerometers, whereas the two headers on the right hand side are the interboard connections. Voltage regulation and brown-out protection is in the lower left hand corner.



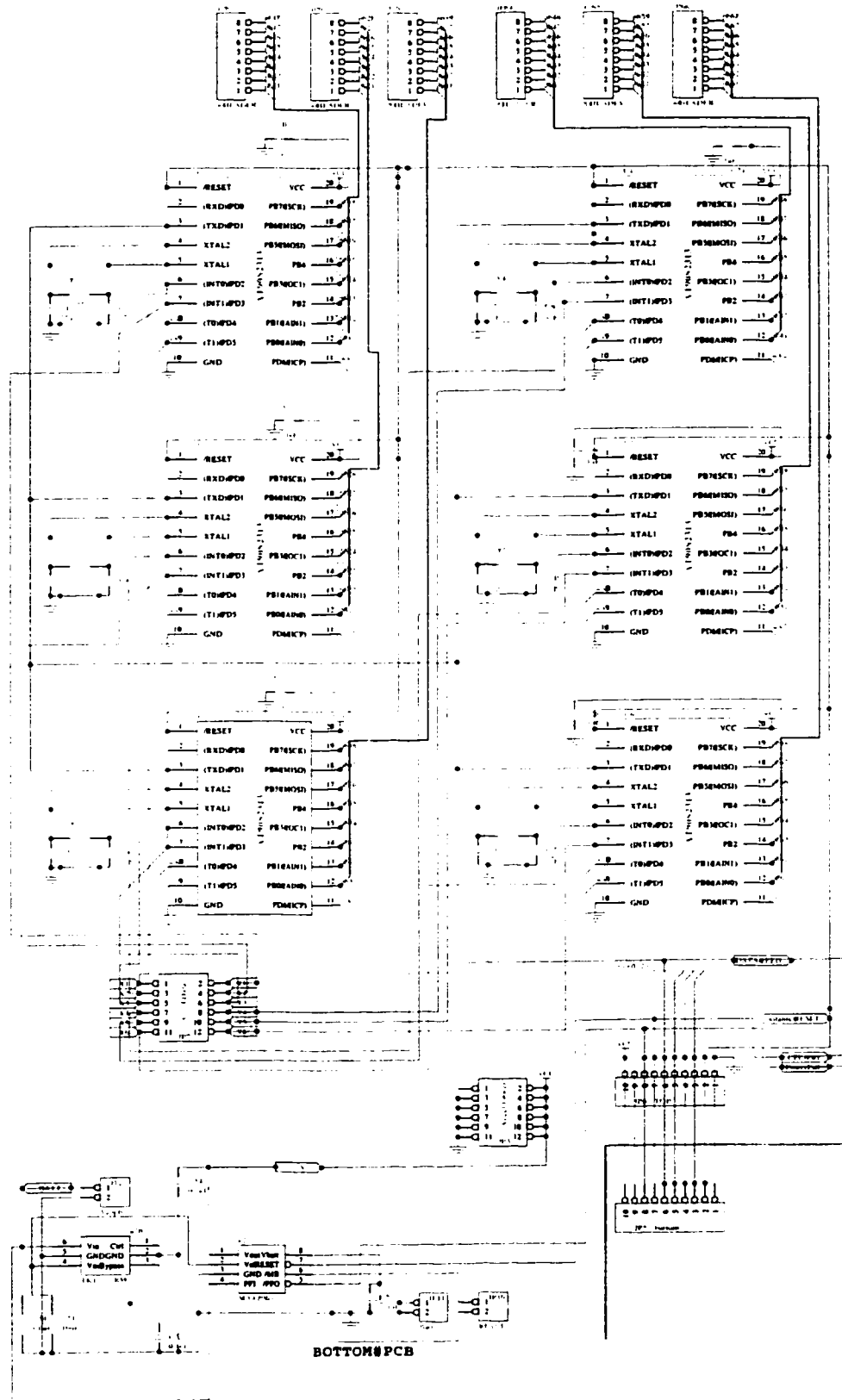


Figure B.1: Schematic of the satellite processors

# Appendix C

## PCB Layout

Figure C.1 is the PCB layout of the master processor / Compact Flash (bottom) and satellite processors (top) board. The footprints for the master processor (ATmega103L) and the Compact Flash connector were created specifically for this system; the remaining footprints were available in the PAD library. The board was manufactured by Alberta Printed Circuits for this research in February of 2001.

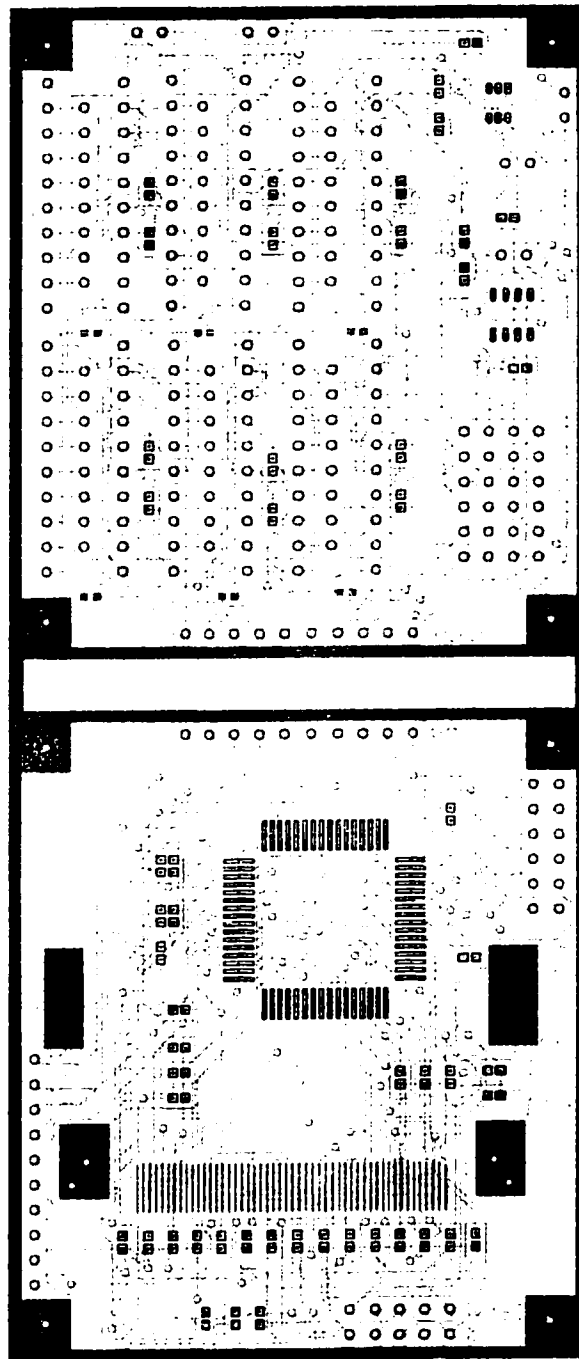


Figure C.1: PCB Layout of Satellite & Master Boards